Published in final edited form as:
Anesth Analg. 2012 May ; 114(5): 1104–1120. doi:10.1213/ANE.0b013e31824b0191.

Prevention of Paclitaxel-Induced Neuropathy Through Activation of the Central Cannabinoid Type 2 Receptor System

Mohamed Naguib, MB, BCh, MSc, FCARCSI, MD,
Institute of Anesthesiology, Cleveland Clinic, Cleveland, Ohio

Jijun J. Xu, MD, PhD,
Institute of Anesthesiology, Cleveland Clinic, Cleveland, Ohio

Philippe Diaz, PhD,

Address correspondence to: Mohamed Naguib, MB, BCh, MSc, FFARCSI, MD Anesthesiology Institute Cleveland Clinic, 9500 Euclid Ave. - NE6-306, Cleveland, OH 44195 Tel (216) 444-6328; Fax (216) 636-2043 naguibm@ccf.org.

See Disclosures at end of article for Author Conflicts of Interest.

Dr. Naguib and Dr. Xu contributed equally to the work.

DISCLOSURES:
Name: Mohamed Naguib, MB, BCh, MSc, FCARCSI, MD
Contribution: This author helped conceptualize the study, design the study, acquire the data, statistical analyses, draft the manuscript, critical revision of the manuscript for important intellectual content, and study supervision.
Conflicts of Interest: Mohamed Naguib is named on two patent applications submitted by the University of Texas MD Anderson Cancer Center.
Name: Jijun J. Xu, MD, PhD
Contribution: This author helped conceptualize the study, design the study, acquire the data, and critical revision of the manuscript for important intellectual content.
Conflicts of Interest: The author has no conflicts of interest to declare.
Name: Philippe Diaz, PhD
Contribution: This author helped conceptualize the study, synthesis of MDA7, and critical revision of the manuscript for important intellectual content.
Conflicts of Interest: Philippe Diaz is named on two patent applications submitted by the University of Texas MD Anderson Cancer Center.
Name: David L. Brown, MD
Contribution: This author helped conceptualize the study, design the study, critical revision of the manuscript for important intellectual content, and study supervision.
Conflicts of Interest: The author has no conflicts of interest to declare.
Name: David Cogdell, MS
Contribution: This author helped acquire the data and critical revision of the manuscript for important intellectual content.
Conflicts of Interest: The author has no conflicts of interest to declare.
Name: Bihua Bie, MD, PhD
Contribution: This author helped acquire the data, technical and material support, and critical revision of the manuscript for important intellectual content.
Conflicts of Interest: The author has no conflicts of interest to declare.
Name: Jianhua Hu, PhD
Contribution: This author helped with statistical analyses.
Conflicts of Interest: The author has no conflicts of interest to declare.
Name: Suzanne Craig, DVM, DACLAM
Contribution: This author helped with the maintenance of the animal colony, technical and material support, and critical revision of the manuscript for important intellectual content.
Conflicts of Interest: The author has no conflicts of interest to declare.
Name: Walter N. Hittelman, PhD
Contribution: This author helped conceptualize the study, design the study, acquire the data, draft the manuscript, critical revision of the manuscript for important intellectual content, and study supervision.
Conflicts of Interest: The author has no conflicts of interest to declare.

The Department of Biomedical and Pharmaceutical, Sciences, Core Laboratory for Neuromolecular Production, The University of Montana, Missoula, Montana

David L. Brown, MD,
Institute of Anesthesiology, Cleveland Clinic, Cleveland, Ohio

David Cogdell, MS,
Department of Pathology Cancer Genomics Core Laboratory, The University of Texas MD Anderson Cancer Center, Houston, Texas

Bihua Bie, MD, PhD,
Institute of Anesthesiology, Cleveland Clinic, Cleveland, Ohio

Jianhua Hu, PhD,
Department of Bioinformatics and Computational Biology, The University of Texas MD Anderson Cancer Center, Houston, Texas

Suzanne Craig, DVM, DACLAM, and
Department of Veterinary Medicine and Surgery, The University of Texas MD Anderson Cancer Center, Houston, Texas

Walter N. Hittelman, PhD
Department of Experimental Therapeutics, The University of Texas MD Anderson Cancer Center, Houston, Texas

Abstract

Background—Peripheral neuropathy is a major dose-limiting toxicity of chemotherapy, especially after multiple courses of paclitaxel. The development of paclitaxel-induced neuropathy is associated with the activation of microglia followed by the activation and proliferation of astrocytes, and the expression and release of proinflammatory cytokines in the spinal dorsal horn. Cannabinoid type 2 (CB_2) receptors are expressed in the microglia in neurodegenerative disease models.

Methods—To explore the potential of CB_2 agonists for preventing paclitaxel-induced neuropathy, we designed and synthesized a novel CB_2-selective agonist, namely MDA7. The effect of MDA7 in preventing paclitaxel-induced allodynia was assessed in rats and in $CB_2^{+/+}$ and $CB_2^{-/-}$ mice. We hypothesize that the CB_2 receptor functions in a negative-feedback loop and that early MDA7 administration can blunt the neuroinflammatory response to paclitaxel and prevent mechanical allodynia through interference with specific signaling pathways.

Results—We found that MDA7 prevents paclitaxel-induced mechanical allodynia in rats and mice in a dose- and time-dependent manner without compromising paclitaxel's antineoplastic effect. MDA7's neuroprotective effect was absent in $CB_2^{-/-}$ mice and was blocked by CB_2 antagonists, suggesting that MDA7's action directly involves CB_2 receptor activation. MDA7 treatment was found to interfere with early events in the paclitaxel-induced neuroinflammatory response as evidenced by relatively reduced Toll-like receptor and CB_2 expression in the lumbar spinal cord, reduced levels of extracellular signal regulated kinase 1/2 activity, reduced numbers of activated microglia and astrocytes, and reduced secretion of proinflammatory mediators *in vivo* and in *in vitro* models.

Conclusions—Our findings suggest an innovative therapeutic approach to prevent chemotherapy-induced neuropathy and may permit more aggressive use of active chemotherapeutic regimens with reduced long-term sequelae.

Introduction

Neuropathic pain, characterized by a reduced nociceptive threshold, persists in the absence of a stimulus and is refractory to traditional analgesics. Cancer patients are at increased risk of neuropathic pain caused by radiotherapy or a variety of chemotherapeutic drugs, including paclitaxel. Paclitaxel has significant clinical activity and is frequently administered in the management of breast, lung, and ovarian cancers;[1] however, its optimal use is limited by its adverse effects, including myelosuppression and peripheral neuropathy. The myelosuppressive side effects have been partially addressed by the use of hematopoietic growth factors (e.g., granulocyte and granulocyte-macrophage colony-stimulating factors) before or after treatment and by altering paclitaxel doses and schedules.[2] Unfortunately, sensory peripheral neuropathy remains a significant long-term problem that limits the amount of paclitaxel treatment that can be administered.[3-5]

Severe peripheral neuropathy (National Cancer Institute Common Toxicity Criteria grade 3 or 4) is dose-dependent and may affect up to 88% of patients receiving paclitaxel-based chemotherapy.[6] In many patients, neuropathic pain persists throughout life and negatively affects physical, emotional, and social quality of life.[7] There is currently no effective symptomatic treatment for paclitaxel-induced neuropathy. Opioids, gabapentin, amitriptyline, and medicinal cannabis preparations have been tried and shown to be ineffective.[8-10] Because treatments for intact neuropathic pain have limitations, there is increasing interest in developing preventive strategies. Several neuroprotective drugs have been tested in animal models and clinical trials for their ability to prevent chemotherapy-associated neuropathy, but these studies have yielded conflicting results.[11-16]

The pathophysiologic underpinnings of peripheral neuropathy are not well understood. Because taxanes cause microtubule stabilization, it has been proposed that taxane-induced peripheral neuropathy might be a direct consequence of microtubular damage. However, peripheral neuropathy also occurs with use of various other chemotherapeutic drugs that have different mechanisms of action, including vinca alkaloids (which destabilize microtubules), cisplatin, oxaliplatin, carboplatin, bortezomib, and thalidomide.[17] Thus, it is hypothesized that peripheral neuropathy is a downstream event that can be initiated by any of a variety of upstream mechanisms.

The upstream initiators of peripheral neuropathy are not well understood; however, the process has the hallmarks of a neuroinflammatory response after innate immune system activation. For example, in the setting of mechanical allodynia associated with nerve transection,[18,19] Toll-like receptors 2 and 4 (TLR2 and TLR4) found on microglia appear to trigger glial activation, initiating proinflammatory and signal transduction pathways[20,21] that lead to the production of proinflammatory cytokines. Similarly, in the setting of paclitaxel treatment, a TLR4-mediated initiating signal[22,23] leads to activation of microglia, activation and proliferation of astrocytes,[24-27] and expression and release of inflammatory cytokines.[28,29] Established mechanical allodynia can be reversed by intrathecally delivered TLR4 receptor antagonists,[30] which prevent transcription factor nuclear factor kappa-light-chain-enhancer of activated B cells activation and TNFα (tumor necrosis factor alpha) overproduction in the spinal cord after sciatic nerve injury.[18]

The endogenous cannabinoid system is a complex system consisting of two cannabinoid (CB) receptors (CB_1—expressed primarily in the brain and CB_2—expressed primarily in the peripheral immune system[31] and in the central nervous system [CNS][32]) seven endogenous endocannabinoid ligands (arachidonic acid derivatives) including anandamide (*N*-arachidonoylethanolamine) and 2-arachidonoylglycerol (2-AG),[33] and several proteins responsible for the regulation of endocannabinoid metabolic pathways, such as

monoacylglycerol lipase and fatty acid amide hydrolase.[34] CB_1 and CB_2 are seven transmembrane, G protein-coupled receptors, and they share 44% overall identity. Both receptors mediate inhibition of adenylyl cyclases and stimulation of mitogen-activated protein kinases (MAPK). Unlike CB_1, CB_2 appears to poorly modulate calcium channels or inwardly rectifying potassium channels.[35] The endocannabinoid 2-AG was found to act as a full agonist (whereas anandamide acts as a weak partial agonist) toward CB_1 and CB_2 receptors.[36,37]

Inflammatory conditions such as Alzheimer's disease[38,39] or peripheral nerve injury[40,41] increase the expression of CB_2 receptors in the CNS. CB_2 receptor agonists have been shown to attenuate allodynia in animal models of formalin intraplantar injection[42] and spinal nerve ligation.[42-44] Microglia express CB_2 mRNA in the spinal cord in the settings of neuropathic pain models, and this expression is colocalized with the activated microglia.[40] While the physiologic role of CB_2 receptors in the neuropathic response is not well understood, they appear to play a crucial role in the negative regulation of central immune response seen with mechanical allodynia induced by sciatic nerve injury in mice.[45] For example, the manifestation of mechanical allodynia was more evident in CB_2 knockout mice than in their wild-type littermates, and mechanical allodynia was attenuated in transgenic mice overexpressing CB_2 receptors.[45] Similarly, *in vitro* CB_2 receptor stimulation suppresses microglial cell activation.[46]

Synthetic Δ^9-tetrahydrocannabinol (Δ^9-THC) analogues (e.g., Marinol®, Cesamet®) and medicinal cannabis preparations containing both Δ^9-THC and cannabidiol (e.g., Sativex®, Cannador®) have been tried clinically in patients with neuropathic pain. However, these drugs in all trials failed to show efficacy compared with placebo, and their use resulted in a high incidence of psychotropic adverse effects.[47-50] In contrast, CB_2 agonists are neuroprotective and are emerging as treatments for neuropathic pain. Moreover, they lack the psychotropic adverse effects normally seen with CB_1 agonists.[42,43,51-53]

To explore the role of CB_2 agonists in preventing neuropathic pain, we designed and synthesized two novel series of CB_2 agonists.[43,54-56] We first assessed the absorption, distribution, metabolism, and excretion and toxicity (ADME-Tox) properties of one of our lead compounds, MDA7.[56] MDA7 was selected for animal studies because it did not show any ADME-Tox–related issues. We then demonstrated the efficacy of MDA7 in ameliorating allodynia induced by either nerve ligation or paclitaxel administration in rats.[43] Moreover, MDA7 caused no impairment of locomotor activities in rats.[43] We therefore tested the hypothesis that MDA7 could prevent paclitaxel-induced allodynia from the outset. It is important to note that our earlier work[43] examined treatment rather than prevention.

In this study, we demonstrate that MDA7 exerts a neuroprotective effect by blunting neuroinflammatory processes that are pivotal for the development of paclitaxel-induced allodynia. We found that MDA7, when given in a time-dependent fashion, can: (i) prevent the development of paclitaxel-induced mechanical allodynia without compromising the antineoplastic effect of paclitaxel; (ii) prevent increases in levels of glial fibrillary acidic protein (GFAP) in astrocytes and of CD11b in microglia (indicative of neuroinflammatory process activation) that are typically seen within the dorsal horn of paclitaxel-treated rats; (iii) down-regulate TLR2 and CB_2 expression in the spinal cord of paclitaxel-treated rats; and (iv) decrease the release of proinflammatory mediators from lipopolysaccharide (LPS)-stimulated primary glial cells *in vitro*. Because CB_2 agonists prevented paclitaxel-induced neuroinflammation and its downstream consequence, mechanical allodynia, we hypothesize that the CB_2 receptor functions in the immunomodulatory negative-feedback loop and that its early activation can blunt neuroinflammatory responses and mechanical allodynia.

Methods

Synthesis and preparation of MDA7

MDA7 was synthesized as described previously[43,56] and was administered in a vehicle consisting of 25% *N*-methylpyrrolidone (International Speciality Products, Wayne, NJ, USA), 25% propylene glycol (The Dow Chemical Company, Midland, MI, USA), 10% Cremophor, EL (BASF, Florham Park, NJ, USA), and purified water (Baxter, Deerfield, IL, USA).

Pharmacokinetics of MDA7

The details of preparation of standard curves, extraction, and quantification of MDA7 in rat plasma and brain tissue are described in the Supplementary Digital Content.

Animals

Adult male Sprague-Dawley rats (Harlan Sprague Dawley, Indianapolis, IN, USA) weighing 120-150 g and male $CB_2^{-/-}$ and $CB_2^{+/+}$ mice weighing 20-25 g were used in experimental procedures approved by MD Anderson's Animal Care and Use Committee. Animals were housed three per cage for rats and five per cage for mice on a 12/12-h light/dark cycle with water and food pellets available ad libitum. We obtained CB_2 knockout ($CB_2^{-/-}$), wild-type ($CB_2^{+/+}$), and $CB_2^{+/-}$ mice from Nancy E. Buckley, PhD, Biological Sciences Department, California State Polytechnic University, Pomona, CA. Mice breeding and genotyping were performed as described by Buckley et al.[57]

Paclitaxel-induced allodynia model

Groups of rats and mice received either vehicle or 1.0 mg/kg of paclitaxel daily i.p. for 4 consecutive days for a final cumulative dose of 4 mg/kg;[58] the injection volume was 1 ml/kg. Baseline responses to mechanical stimulation of the hindpaw (see below) were established on day 0 and continued for 28 days as described later. The behavioral testing was performed blindly with respect to the drug administration.

Assessment of mechanical withdrawal thresholds

Rats or mice were placed in a compartment with a wire mesh bottom and allowed to acclimate for 30 min before testing. Sensory thresholds for the development of allodynia to mechanical stimuli were assessed. Mechanical sensitivity was assessed by using a series of Von Frey filaments with logarithmic incremental stiffness (Stoelting Co., Wood Dale, IL, USA), as previously described,[59] and 50% probability paw withdrawal thresholds were calculated with the up-down method.[60] In brief, filaments were applied to the plantar surface of a hindpaw for about 6 s in an ascending or descending order after a negative or positive withdrawal response, respectively. Six consecutive responses after the first change in response were used to calculate the paw withdrawal threshold (in grams). In rats, when response thresholds occurred outside the range of detection, the paw withdrawal threshold was assigned at 15.00 g for continuous negative responses and at 0.25 g for continuous positive responses. Corresponding values in mice were 2.5 g and 0.02 g, respectively.[61] No rats or mice died during treatment or showed evidence of illness.

Immunohistochemical analysis

Animals were deeply anesthetized with 2-4% isoflurane in oxygen and perfused transcardially with heparinized normal saline (150 ml) followed by 4% formaldehyde (250 ml) and 10% sucrose (200 ml), both in 0.1 M phosphate buffered saline (PBS), at room temperature. Spinal cords were quickly extruded through a cervical cut by high-pressure injection of ice-cold saline via a needle inserted intrathecally at the level of the cauda

equina. The lumbar spinal cords were quickly postfixed in 4% formaldehyde and cryopreserved in 30% sucrose in PBS for 48-72 h at 4°C. The spinal cord tissues were then cut to 25 μm in thickness and collected free-floating in 0.1 M PBS. Tissue sections were washed with 0.1% Triton-X 100 in PBS and blocked with donkey or goat serum (according to the secondary antibodies used later) followed by washing with PBS. Primary antibodies (GFAP to label astrocytes: 1:5000, Millipore, Billerica, MA; CD11b [a complement receptor 3 antigen recognized by the OX42 antibody] to label microglial cells: 1:200, Millipore, Billerica, MA; CB_2 rabbit polyclonal antibody immunoglobulin G (the immunogen is a fusion protein containing the first 32 amino acid residues from rat CB2; Catalog number: PA1-746A), 1:500, Affinity BioReagents, Golden, CO; phosphor-p38 MAPK, Cell Signaling, Beverly, MA) were applied to the sections for 2 h at room temperature and then overnight at 4°C. Sections were washed with PBS and incubated with fluorescein isothiocyanate or Cy3 (as indicated in colocalization study) conjugated secondary antibodies (Jackson Immuno Laboratories, West Grove, PA, USA) for 2 h at room temperature. Sections were then rinsed with wash buffer and mounted with SlowFade antifade reagents (Invitrogen, Carlsbad, CA, USA).

Confocal imaging and image analyses

Immunostained tissue sections were imaged by using a Zeiss LSM 510 inverted confocal microscope (Carl Zeiss Microimaging, Inc., Thornwood, NY, USA) with either a 40× or a 25× oil immersion objective. Images were obtained through the full thickness of the tissue section by using fixed serial optical slices along the z-axis, laser power, and detector/amplifier settings for all treatment conditions to permit quantitatively comparable images for all treatment conditions. For both microglial and astrocytic cell activation, the staining intensities were examined in a standardized area of laminae I–II with 3-5 slices examined per animal. The exposure and capture conditions for each channel were adjusted to ensure that images were captured within the dynamic range for all samples. Fluorescence image stacks were quantified for both fluorescence intensity and relative area occupied by labeled objects by using two separate methodologies. Negative control sections processed with the secondary antibody alone were used to account for the autofluorescence from the spinal cord itself and nonspecific fluorescence from secondary antibody. First, using Zeiss LSM 3-dimensional software, a specific number of sections was maximally projected. The relative area occupied by the fluorescence objects was then quantified on thresholded projected images. The threshold was set to two standard deviations above the control signals. Second, the images were exported in a .tif format into MetaMorph software (Molecular Devices, Downingtown, PA, USA). Multiple representative sections (every five optical slices) from each image stack were quantified for total fluorescence intensity and percentage thresholded area after the background fluorescence was subtracted. The stack projections were also quantified for integrated fluorescence and percentage thresholded area. Glial activation is characterized by an increase in the number and complexity of these cells (rounded cell bodies and thicker processes), resulting in an increase in “labeling.” The pseudocolored representations of the spatial distributions of fluorescence shown in Supplemtnal Digital Content Fig. 3 was used to better define morphological changes. Therefore, an increase in the number of pixels above the threshold value was a measure of glial activation.

Gene expression profiling studies

Total RNA was extracted from spinal cord samples by using *mir*Vana RNA isolation kits (Ambion, Austin, TX, USA), according to the manufacturer's recommendations. The quality of RNA was analyzed by using a Nanodrop spectrophotometer (Wilmington, DE, USA) and microfluidic gel station (Agilent 2100 Bioanalyzer, Santa Clara, CA, USA). The wavelength 260/280 ratio was >1.8 with RNA integrity number >9. The whole-genome rat gene expression profiling experiments were performed by using 44K-long oligonucleotide

microarrays from Agilent Biotechnology. Differentially expressed gene lists were generated from spinal cord samples of each experimental rat by using Agilent software after normalization.

The within-array loess normalization was implemented on the logarithm-2 transformed ratio of cyanine 5 to cyanine 3 signals to diminish the systematic bias that resulted from dye effect and other factors.[62] We conducted the one-sample t-test on the treatment effect for a gene. Explicitly, a nontrivial positive treatment effect indicates up-regulation with MDA7 and paclitaxel treatment, and *vice versa*. We adopted a false discovery rate, widely used in microarray experiments, to control multiple testing error rates.[63,64] The false discovery rate is the percentage of false-positives among all genes identified as being differentially expressed between two treatments. The beta-uniform mixture model[65] was used to determine the *P*-value threshold based on the false discovery rate.

Quantitative real-time reverse transcriptase-polymerase chain reaction (qRT-PCR)

To determine fold-changes in RNA samples, 1.0 μg of total RNA was reverse-transcribed in a 20 μl reaction. Maintaining a ratio of 1 μg total RNA to 0.4 μg of random hexamers, random hexamers were added and the mixture was heated at 70°C for 10 min. The tubes were then incubated at room temperature for 10 min, and the following components were added: 1X Superscript II RT Buffer (Invitrogen), 10 mM DTT (Invitrogen), 0.5 mM dNTP's (ISC Bioexpress, Kaysville, UT, USA), 20U RNase Inhibitor (Ambion), and 200U Superscript II Reverse Transcriptase (Invitrogen). The reaction was incubated for 10 min at room temperature and then held at 37°C for 1 h. The reaction was then incubated at 42°C for 1.5 h followed by 50°C for 30 min. RT PCR was performed on the ABI Prism 7900 by using the Assays-on-Demand (4331182) for interleukin (IL)-1β (Rn00580432_m1), TNFα (Rn99999017_m1), Cyp26b1 (Rn00710376_m1), Pofut2_predicted (Rn01429345_m1), Cst3 (Rn01415507_g1), Kcns3 (Rn00696209_m1), Akr7a3 (Rn00566256_m1), and the Rat GAPD (4352338E). Vic-labeled Pre-Developed Assay Reagent (Applied Biosystems, Foster City, CA, USA) was used without multiplexing using a 15 μl final reaction volume containing 1X TaqMan Universal PCR Master Mix (Applied Biosystems) and 1X Assay-on-Demand. A total of 2.5 ng/well cDNA was amplified with the following cycling conditions: 10 min at 95°C followed by 50 cycles of 95°C for 15 s and 60°C for 1 min. The 7900 Sequence Detection System 2.3 software automatically determined fold-change for each sample using the ΔΔCt method with 95% confidence.

Cell cultures

Primary astroglial cell culture—Astrocyte-enriched cultures were prepared from cerebral cortices of 2 or 3-day-old Sprague-Dawley rats with few modifications to the method previously described.[66] In brief, rats were decapitated and cerebral cortices immediately dissected out. After meninges and blood vessels were removed, the tissues were minced and washed in PBS and then incubated for 30 min at 37°C in 0.25% trypsin-EDTA (Sigma, St. Louis, MO, USA). Cells were then mechanically triturated through a glass pipette and filtered through a 70-μm nylon mesh in the presence of 10% fetal bovine serum (FBS) in Dulbecco's modified Eagle's medium (DMEM):F12 (MediaTech, Manassas, VA, USA) and 15,000 IU/ml DNase I (Sigma). After centrifugation (500 g), cells in 90% DMEM, 10% FBS, 20 U/ml penicillin, and 20 μg/ml streptomycin were seeded in plastic Petri dishes or cell culture plates (BD Falcon, Franklin Lakes, NJ, USA) at 1.25×10^5 cells/cm^2. Cells were maintained in a humidified atmosphere of 90% air-10% CO_2. The medium was changed once a week, and cells were used after 14-19 days in vitro.

CHO-CB_2 and HEK-293-TLR cell culture—The rCB_2- or hCB_2- transfected Chinese hamster ovary (CHO) cells were cultured in HAM-F12 medium (MediaTech) containing

10% FBS (Sigma), 100 IU/ml penicillin, 100 μg/ml streptomycin, and 400 μg/ml G418. The TLR2 or TLR4 transfected Human Embryonic Kidney (HEK) cells were purchased from InvivoGen (San Diego, CA) and cultured in DMEM containing 10% FBS, 100 IU/ml penicillin, 100 μg/ml streptomycin, and 100 μg/ml each of Normocin and HEK-Blue selection (antibiotics for maintenance of the transfected cells, both from InvivoGen), according to the manufacturer's instructions.

Western blotting

Western blotting in lumbar spinal cord tissue—Groups of rats were injected with paclitaxel at 1 mg/kg for 4 days, or paclitaxel for 4 days plus 15 mg/kg MDA7 (15 min before paclitaxel) for 4 or 14 days. Animals were deeply anesthetized with 2-4% isoflurane in oxygen and perfused transcardially with normal saline (150 ml). Spinal cords were quickly extruded through the cervical cut by high-pressure injection of ice-cold saline via a needle inserted intrathecally at the level of the cauda equina. The lumbosacral enlargement was excised and if not studied immediately afterward, was frozen on dry ice and stored at –80°C until assayed. Lumbar spinal tissues were homogenized and sonicated in buffer 1.0% Nonidet P-40, 20 mM Hepes (pH 7.5), 150 mM NaCl, 10% glycerol, 60 mM octyl β-glucoside, 10 mM NaF, 1.0 mM Na3VO4, 2.5 mM nitrophenylphosphate, 1 mM phenylmethylsulfonyl fluoride, 0.7 μg/ml of pepstatin, and a protease inhibitor cocktail tablet (Roche, Mannheim, Germany), and centrifuged at 12,000 rpm at 4°C for 15 min. The supernatants (lysate) were collected. From the lysate, total protein was taken and dissolved in 2× Laemmli buffer. The samples were separated by sodium dodecyl sulfate–polyacrylamide gel electrophoresis and then transferred onto nitrocellulose membranes (Whatman Inc.). Antibodies against CB_2 (1:500, Affinity BioReagents), extracellular signal regulated kinase (ERK)1/2 and phosphorylated-ERK1/2 (1:1500, Cell Signaling), IkBα and phosphorylated-IkBα (1:1000, Cell Signaling), TLR2 (1:500, Imegenex, San Diego, CA, USA) and TLR4 (1:500, Imegenex), and β-actin (1:1000, Cell Signaling) were used as the primary antibodies.

Western blotting in CHO-CB_2 and HEK-293-TLR cell cultures—Cells were treated with dimethylsulfoxide (DMSO) (vehicle) and 0.1 μM paclitaxel (15 min) with or without 1 and 10 μM MDA7 (1 h before paclitaxel). Antibodies to ERK1/2 and phosphorylated-ERK1/2 (1:1500, Cell Signaling) were used as the primary antibodies. Cells were lysed and sonicated in buffer (1.0% Nonidet P-40), 20 mM Hepes (pH 7.5), 150 mM NaCl, 10% glycerol, 60 mM octyl β-glucoside, 10 mM NaF, 1.0 mM Na_3VO_4, 2.5 mM nitrophenylphosphate, 1 mM phenylmethylsulfonyl fluoride, 0.7 μg/ml of pepstatin, and a protease inhibitor cocktail tablet (Roche, Mannheim, Germany) and centrifuged at 12,000 rpm at 4°C for 15 min. The supernatants (lysate) were collected. From the lysate, total protein was taken and dissolved in 2× Laemmli buffer. The samples were separated by sodium dodecyl sulfate–polyacrylamide gel electrophoresis and then transferred onto nitrocellulose membranes (Whatman Inc., Florham Park, NJ, USA). β-actin was used as loading control. Band analysis (quantification) was conducted by using Alpha Innotech FluorChem FC12 software (San Leandro, CA, USA).

Measurement of cytokine production in the cultured astroglial cells (enzyme-linked immunosorbent assay analysis)—The primary astroglial cultured cells were treated with 5 μM DMSO (solvent), 1.0 μg/ml of LPS,[67] and 100 μg/ml zymosan with or without 10 μM MDA7. Cell culture supernatants were collected 24 h after treatment. IL-1β and TNFα were quantified by using commercial enzyme-linked immunosorbent assay (ELISA) kits from R&D Systems (Minneapolis, MN) with a sensitivity of less than 5 pg/ml. Experiments were performed in triplicate.

Flow cytometric analysis—The quantification of an apoptotic response was performed using an LSR Flow Cytometer (Becton-Dickinson, Franklin Lakes, NJ). By conjugating fluorescein isothiocyanate (FITC) to Annexin V, it is possible to identify and quantitate apoptotic cells on a single-cell basis by flow cytometry. Staining cells simultaneously with FITC-Annexin V and PI allows (bivariate analysis) the discrimination of viable cells (Annexin V-FITC and PI negative), early apoptotic cells (Annexin V-FITC positive and PI negative), and late apoptotic or necrotic cells (both Annexin V-FITC and PI positive).

Statistics—For behavioral data in rats, linear mixed models[68] with treatment and day effects with repeated measures over days were used to assess whether MDA7 significantly prevented paclitaxel-induced allodynia. In the mice study, a linear mixed model with a random intercept effect was used to account for the dependent measurements over time. This model includes the genotype, time, and interaction between genotype and time as the fixed effect. This model allows assessing the baseline effect, the time effect and the difference between the genotypes in terms of the change over time. The quadratic term of time is included if the change of the measurements over time is nonlinear. We used a two-way ANOVA model to compare the baseline measurements between the two mice genotypes (at day 0). Immunohistochemistry and immunoblots data were analyzed by using the *t*-test or two-way ANOVA followed by post hoc Student–Newman–Keuls test. All data are expressed as mean ± SEM. $P<0.05$ was considered statistically significant.

Results

Administration of MDA7 effectively prevents paclitaxel-induced allodynia through the CB2 receptor system

Tactile allodynia (pain induced by tactile stimulation that is not normally painful) is a clinically important component of neuropathic pain and is commonly considered as a primary endpoint in neuropathic pain models. To develop a rat model for studying mechanical allodynia after paclitaxel treatment, we administered 1 mg/kg of paclitaxel intraperitoneally (i.p.) in rats for 4 consecutive days.[43,58] This resulted in the development of tactile allodynia in all of the rats, as shown by a reduction in paw withdrawal threshold to mechanical stimulation with von Frey filaments, from 14.4 ± 0.6 g before the start of paclitaxel administration to 2.1 ± 0.3 g by day 8 after administration. This paclitaxel-induced allodynia persisted throughout the 28-day study period (Fig. 1).

To determine whether MDA7 could prevent paclitaxel-induced allodynia and exert a neuroprotective effect, we administered 15 mg/kg of MDA7 i.p. 15 min before each paclitaxel dose for 4 days and then continued daily MDA7 administration for another 10 days (total period of MDA7 treatment: 14 consecutive days). This schedule of MDA7 treatment prevented paclitaxel-induced allodynia in all rats; the protective effects lasted throughout the study period (4 days during and 24 days after paclitaxel administration) (Fig. 1). In contrast, MDA7 (15 mg/kg i.p.) given 15 min before the paclitaxel administration for only the first 4 days of paclitaxel administration delayed but did not prevent paclitaxel-induced allodynia. This result suggests that MDA7 treatment does not directly interfere with paclitaxel action and that the downstream effects of paclitaxel treatment can still be elicited over a window of time after discontinuation of paclitaxel treatment.

Because MDA7 was designed as a CB_2 agonist, it was important to determine whether the observed protective effects of MDA7 were directly mediated through CB_2 receptor activation. We therefore administered 5 mg/kg i.p. of AM630, a CB_2 antagonist, to rats before MDA7 (15 mg/kg i.p.) administration. This abolished the protective effects of MDA7 (Fig. 1). To further explore whether the neuroprotective effect of MDA7 directly involved CB_2 receptor activation, we performed parallel studies in mice lacking the CB_2 receptor.

Interestingly, $CB_2^{-/-}$ mice were inherently more sensitive ($P = 0.005$) to tactile stimulation than $CB_2^{+/+}$ mice at the outset of the experiment and had a more rapid onset ($P = 0.019$) of allodynia after paclitaxel administration, suggesting that the $CB_2^{-/-}$ mice exhibit a presensitization syndrome and are prone to more severe allodynia. Of note, MDA7 was shown to protect $CB_2^{+/+}$ mice but not $CB_2^{-/-}$ mice from paclitaxel-induced allodynia (Fig. 2). These parallel studies in rats and mice strongly support the notion that the protective effect of MDA7 was mediated through the CB_2 receptor.

Pharmacokinetics of MDA7

An important observation from the above experiment was that, while a 4-day MDA7 treatment only delayed (but did not prevent) paclitaxel-induced allodynia, a 14-day course provided a neuroprotective effect that lasted long after MDA7 administration was discontinued. There could be two explanations for this observation: the therapeutic concentrations of MDA7 may require more than 4 days; or, there is a window of therapeutic opportunity for MDA7's protective effect. To better understand this phenomenon, we determined the pharmacokinetics of MDA7 in rats in both the plasma and the CNS. As illustrated in Supplemental Digital Content Figure 2, IV administration of MDA7 achieved a CNS concentration (C_{max} of 15 μg/g) that was 3 times larger than that simultaneously measured in plasma; however, the MDA7 concentration decreased to less than 0.1 μg/ml within 4 h.

MDA7 effectively ameliorates the activation of spinal astrocyte and microglia induced by paclitaxel

Because prior studies showed an association between the development of mechanical allodynia and glial cell activation,[69,70] we considered the possibility that MDA7's preventive effect on paclitaxel-induced allodynia in rats was mediated through modulation of glial activation. Increased expression of specific markers such as CD11b and GFAP have been associated with activation of microglia[71] and astrocytes,[72] respectively. We therefore examined the impact of MDA7 on paclitaxel-induced microglial and astrocyte activation by comparing the levels of immunofluorescence staining for CD11b and GFAP in the dorsal horn laminae I and II of the lumbar spinal cord of rats in the various treatment groups tested shown in Fig. 1 (on day 28). Glial activation is characterized by an increase in the number and complexity of these cells (rounded cell bodies and thicker processes), resulting in an increase in both the number of labeled cells and the total integrated intensity of the labeled cells (Supplemental Digital Content Fig. 3). When rat lumbar spinal cords were examined on day 28, profoundly increased CD11b and GFAP immunoreactivity, enlarged cell mass and increased cell complexity were noted in the microglia (Fig. 1B and 1C) and astrocytes (Fig. 1D and 1E) of paclitaxel-treated rats. These changes were strongly attenuated in paclitaxel-treated rats receiving 14 days of MDA7 treatment (Fig. 1B, 1C, 1D, and 1E) and correlated well with the effect of MDA7 in preventing mechanical allodynia in the rats (Fig. 1A).

We also found that CB_2 expression was enhanced with paclitaxel administration ($F_{(1,10)} = 13.69$, n =12, $P<0.01$ *versus* control group) and that this expression is colocalized with the reactive astrocytes. Administration of paclitaxel and MDA7 for 14 days resulted in reduced CB_2 expression present at day 28 (Fig. 3, $F_{(1,10)} = 10.65$, n =12, $P<0.01$ *versus* paclitaxel group). Interestingly, the microglial activation marker CD11b was significantly increased ($P < 0.001$) in paclitaxel-treated rats after MDA7 treatment for only 4 days compared with paclitaxel treatment only (Fig. 1B and 1C). Conversely, the astrocytic activation marker GFAP showed the opposite pattern when measured at day 28 (Fig. 1D and 1E).

Molecular pathway of paclitaxel-induced allodynia and its modulation by MDA7

To gain insight into the molecular pathways involved in the development of paclitaxel-induced allodynia and its prevention by MDA7, we performed a second independent experiment similar to that described in Fig. 1 except that the animals were euthanized on day 15 (one day after the last MDA7 dose). Total RNA was extracted from spinal cord samples of rats treated with paclitaxel (1 mg/kg i.p. daily for 4 days) or paclitaxel (1 mg/kg i.p. daily for 4 days) + MDA7 (15 mg/kg i.p. daily for 14 days) (n = 6 in each group). Whole-genome rat gene expression profiling experiments were performed by using rat 44K Agilent Biotechnology (Santa Clara, CA) long oligonucleotide microarrays. While some variation was observed between similarly treated rats (Fig. 4A), we detected 384 genes that had significantly differential expression between paclitaxel-treated rats that did or did not receive MDA7, with $P<1.74 \times 10^{-4}$ based on the false discovery rate cutoff of 0.005 (Fig. 4A and Supplemental Digital Content Table 1). There were 96 genes differentially decreased in expression and 288 genes differentially increased in expression between the two groups. Microarray expression data from all spinal cord samples were validated at the protein level by Western blotting (Fig. 4C-4H) or at the RNA level by quantitative qRT-PCR (Fig. 4B) based on an examination of 7 gene products selected for their known involvement in inflammatory pathways, including : (i) protein-o-fucosyltransferase 2 (Pofut2_predicted), an essential component of the Notch signaling pathway[73,74] which is involved in neuronal and glial differentiation and modulation of the expression of proinflammatory cytokines:[75,76] 1.9 fold difference; (ii) Cyp26b1, a regulator of retinoic acid oxidation associated with human CNS development:[77] 1.8 fold difference; (iii) IL-1β: 1.2 fold difference; (iv) tumor necrosis factor-α (TNFα): 1.2 fold difference; (v) TLR2: 1.3 fold difference; (vi) IκBα: 1.3 fold difference; and (vii) ERK1 and ERK2, activated in the microglia within 1-3 days and in astrocytes after 3 weeks in the neuropathic spinal nerve ligation model: 1.22 and 1.04 fold changes, respectively. These qRT-PCR results yielded the same trends as those obtained from the microarray analyses. Moreover, at the protein level, paclitaxel treatment alone was associated with upregulated TLR2 expression ($F_{(1,8)}$=12.1, n =10, P<0.05) and increased phosphorylation of ERK1/2 ($F_{(1,8)}$=7.9, n = 10, P<0.05) and IκBα ($F_{(1,8)}$=11.1, n = 10, P<0.05) in the rat spinal cord (Fig. 4C-H). MDA7 treatment for 14 days significantly attenuated the upsurge of phosphorylation of ERK1/2 (Fig. 4C, D) ($\boldsymbol{F}_{(1,8)}$ = 8.36, n =10, P<0.05) and IκBα (Fig. 4E, F) ($\boldsymbol{F}_{(1,8)}$ = 8.35, n = 10, P<0.05), and down-regulated TLR2 expression (Fig. 4G,H) ($\boldsymbol{F}_{(1,8)}$ = 8.11, n = 10, P<0.05) but did not affect TLR4 (Fig. 4G, H) ($\boldsymbol{F}_{(1,6)}$ = 0.25, n = 8, P>0.05) expression in the lumbar spinal cord of the rats with paclitaxel treatment.

MDA7 attenuates proinflammatory cytokine secretion induced by LPS and Zymosan via suppression of ERK1/2 signaling in primary cultured astroglial cells

To better understand the basis for MDA7's interference with paclitaxel-induced allodynia, we examined the impact of MDA7 treatment on proinflammatory cytokine secretion by cultured astroglial cells that express TLRs.[78] LPS (a ligand for TLR4)[79] and zymosan (a ligand for TLR2)[80] elicit the secretion of proinflammatory cytokines in this model system. Prior studies indicated the involvement of TLR4 signaling in both paclitaxel- and LPS-induced signaling pathways.[81] LPS has also been shown to increase CB_2 receptor levels.[82] As shown in Figure 5A and 5B, secreted levels of IL-1β and TNF-α were significantly increased in primary rat astroglial cell cultures after 1.0 μg/ml LPS or 100 μg/ml zymosan stimulation, and these increases were blunted by MDA7 treatment. Pretreatment with MDA7 significantly inhibited LPS-induced increases in IL-1β (Fig. 5A, $F_{(1,8)}$ = 28.38, n =10, P<0.001) and TNF-α secretion (Fig. 5B, $F_{(1,5)}$ = 64.41, n = 7, P<0.001). Similarly, it also suppressed zymosan-induced increases in IL-1β (Fig. 5A, $F_{(1,6)}$ = 8.07, n = 8, P<0.05) and TNF-α secretion (Fig. 5B, $F_{(1,4)}$ = 506.03, n = 6, P<0.001). Treatment of these primary astroglial cultures with 0.1 μM paclitaxel was associated with increased TLR2 (but not

TLR4) gene expression (Fig. 5C, $F_{(1,4)}$ =11.08, n = 6, P<0.05), but paclitaxel alone failed to induce IL-1β and TNF-α production in this in vitro model (data not shown), suggesting that paclitaxel treatment itself may not cause TLR2 or TLR4 activation similar to that induced by LPS or zymosan. Of interest, the increase in TLR2 gene expression associated with paclitaxel treatment was suppressed by MDA7 treatment (Fig. 5C, $F_{(1,4)}$ =14.00, n = 6, P<0.05), suggesting that MDA7 can impact an early component of paclitaxel-induced signaling pathways.

MDA7 suppresses paclitaxel-induced ERK1/2 activation in CHO-CB_2 and HEK-TLR2/4 cells

We determined the effect of MDA7 on ERK phosphorylation in human CB_2 (*h*CB_2)-transfected or rat CB_2 (*r*CB_2)-transfected CHO cells and in TLR2- or TLR4-transfected HEK-293 cells after paclitaxel treatment.[83] Supplemental Digital Content Figure 4 shows that TLR-transfected HEK-293 cells express CB_2 receptors. We noted that both endogenous ERK1/2 phosphorylation (in CB_2–transfected cells) and paclitaxel-induced ERK1/2 phosphorylation were suppressed by MDA7 (Fig. 6) in a dose-dependent fashion. Treatment with MDA7 significantly suppressed phosphorylation of ERK1/2 in TLR2- ($F_{(1,4)}$ = 8.56, P<0.05) or TLR4- ($F_{(1,4)}$ = 19.97, P=0.01) transfected HEK-293 cells when compared to paclitaxel-treated cells. Although paclitaxel has been shown to induce ERK1/2 phosphorylation,[84] our data show that the effect of paclitaxel on ERK1/2 phosphorylation did not differ significantly from controls in TLR 2- ($F_{(1,4)}$ = 0.33, n = 6, P = 0.32) or in TLR4- ($F_{(1,4)}$ = 5.15, n = 6, P = 0.08) transfected HEK-293 cells (Fig. 7). This MDA7-induced effect can be blocked by a CB_2 antagonist (AM630), as demonstrated in the TLR-transfected HEK-293 cells and CB_2-CHO cells shown in Supplemental Digital Content Fig. 5. Recently, it has been shown that AM630 behaves as a protean ligand at the *h*CB_2 receptor.[85] Depending on the cell context, a protean agonist ligand can be an agonist, neutral antagonist, or inverse agonist at the same receptor type. Therefore, the effect of AM630 on the levels of pERK in both CHO-CB2 cells and HEK-TLR2 cells is not unexpected (Supplemental Digital Content Fig. 5). These data indicate that MDA7 treatment can reduce p-ERK1/2 signaling at an early stage in the neuroinflammatory process and potentially blunt downstream pathways that generate allodynia.

Administration of MDA7 did not interfere with paclitaxel's activity in various human cancer cell lines

If MDA7 is to be indicated for the prevention of peripheral neuropathy in the chemotherapy setting, it is important that MDA7 not compromise the cytotoxic effects of paclitaxel on tumor cells. To address this issue, we determined the effect of MDA7 on paclitaxel-induced cell death in various human cancer cell lines, including MCF7 breast adenocarcinoma, H1299 lung cancer, and Jurkat leukemia cells. The addition of MDA7 to paclitaxel during a 24-h (data not shown) or a 48-h treatment did not compromise the ability of paclitaxel to induce a necrotic (propidium iodide uptake) or apoptotic (Annexin staining) reaction (Fig. 8). In fact, MDA7 itself increased cell death in MCF7 cells above control levels. These results are consistent with prior studies demonstrating antiproliferative effects of CB_2 agonists on a wide spectrum of tumor cells[86,87] and further supports MDA7's potential indication for preventing mechanical allodynia in the chemotherapy setting.

Discussion

Our results reveal a promising potential role for the CB_2 agonist MDA7 in preventing paclitaxel-induced mechanical allodynia. Our preclinical data indicate that MDA7 prevented paclitaxel-induced allodynia in rats and in $CB_2^{+/+}$ mice, perhaps by upregulating an immunomodulatory negative feedback loop early during a paclitaxel-induced neuroinflammatory reaction. The *in vivo* studies demonstrated that paclitaxel treatment

resulted in activation and expansion of microglia and astrocytes in the spinal cord, a process that was blunted by MDA7 treatment. Similarly, concomitant treatment of paclitaxel-treated animals with MDA7 was associated with decreased expression of genes involved with the neuroinflammatory response. The *in vitro* studies further demonstrated that MDA7 treatment could attenuate activation of early signaling pathways associated with the neuroinflammatory pathway by interfering with paclitaxel-induced TLR2 upregulation and ERK1/2 phosphorylation, and this was associated with decreased secretion of proinflammatory cytokines (e.g., IL-1β and TNF-α). The finding that paclitaxel treatment was associated with increased CB_2 expression in the dorsal horn laminae I and II lumbar spinal cord in paclitaxel-treated rats (Fig. 3), yet treatment with the CB_2 agonist MDA7 prevented the development of mechanical allodynia, raises the possibility that the CB_2 receptor acts as a negative feedback regulator and its early activation by MDA7 can serve to limit the extent of the neuroinflammatory response and the subsequent development of allodynia. Moreover, by blunting the development of paclitaxel-induced microgliosis in the spinal cord, early MDA7 treatment may result in reduced sensitization for subsequent paclitaxel courses.

Administering 15 mg/kg i.p. of MDA7 15 min before administering paclitaxel for 4 days and then continuing the MDA7 for another 10 days (total period of MDA7 administration: 14 consecutive days) prevented paclitaxel-induced allodynia in rats and in $CB_2^{+/+}$ mice but not in $CB_2^{-/-}$ mice. These findings suggest that (i) the presence of the CB_2 receptor is critical for the neuroprotective activity of MDA7; and (ii) MDA7 itself does not directly interfere with paclitaxel activity. Administering 15 mg/kg i.p. of MDA7 for only the first 4 days of paclitaxel administration delayed but did not prevent paclitaxel-induced allodynia. This suggests that: (i) there is a window of preventive opportunity where CB_2 agonists have maximal activity; and (ii) the upstream signal initiating paclitaxel-induced allodynia is transitory in nature and that continued effective concentrations of MDA7 need to be present in the CNS during this interval to effectively block this neuroinflammatory-initiating signal.

Our *in vivo* analyses showed that the level of microglial activation marker CD11b (measured on day 28) was significantly higher ($P < 0.001$) after MDA7 treatment for 4 days than it was after paclitaxel treatment alone (Fig. 1B and 1C); yet the astrocytic activation marker GFAP showed an opposite pattern (Fig. 1D and 1E). This suggests that the microglia are involved in the initiating phase of behavioral hypersensitivity, whereas astrocytes are involved in the maintenance phase.[88-90] This notion is supported by observations of others that microglial cells begin to retract their fine ramifications, enlarge, and enter mitosis within 24 h after axotomy, later followed by astrocyte activation.[88] Our results are consistent with previously published reports in which a similar dosing regimen of paclitaxel resulted in mechanical allodynia[43,58,91,92] and microglial activation.[93] Zheng et al.,[94] however, failed to demonstrate microglial activation after paclitaxel administration perhaps due to measuring a different endpoint of markers or the use of a high threshold for their measurements.

The present studies provide some insight into the mechanism by which this CB_2 agonist, MDA7, blunts the paclitaxel-induced neuroinflammatory response associated with mechanical allodynia. Signaling via TLRs is thought to mediate the expression of a wide array of genes involved in inflammatory and immune responses.[95] Although TLRs appear to be differentially up-regulated in stimulated microglia in different stimulatory settings,[96] TLR2 has been reported to be involved in glial cell activation associated with models of neuropathic pain.[21,97] The finding that MDA7 has a relatively short half-life suggests that its protective mechanism might involve an inhibition of a TLR activation pathway (e.g., binding to TLR and preventing TLR dimerization necessary for activation) rather than a competitive pathway (which might require chronic administration). Both spinal cord

microglia activation and proinflammatory gene expression in the spinal cord (such as TNFα and IL-1β) induced by nerve injury were reduced in TLR2 knockout mice.[97] Our finding of relatively reduced paclitaxel-induced TLR2 expression levels along with decreased ERK1/2 phosphorylation in MDA7-treated animals and decreased secretion of inflammatory cytokines in MDA7-treated cells *in vitro* suggest that MDA7 treatment modulates early events in the paclitaxel-induced neuroinflammatory response underlying the development of mechanical allodynia.

ERK regulates a wide spectrum of cell functions and has been shown to play an important role in tissue and nerve injury[98,99] and pain sensitization.[100] After nerve injury, ERK1/2 is differentially activated (phosphorylated) in spinal glial cells.[101] Moreover, inhibition of ERK pathways has been shown to attenuate TNF production[102] and mechanical allodynia in different animal models.[99] However, current ERK inhibitors have poor CNS penetration characteristics and have not proven beneficial in preclinical trials because of their toxicity and limited efficacy.[103] Anandamide has been shown to modulate ERK1/2 activation within the CNS immune system, to reduce the extent of the inflammatory response, and to limit neurodegenerative immune reactions.[104] Our data indicate that MDA7 treatment can reduce phosphorylated ERK1/2 signaling at an early stage in the neuroinflammatory process and potentially blunt downstream pathways that generate allodynia.

Taken together, our data suggest that paclitaxel treatment initiates a neuroinflammatory process in the spinal cord characterized by increased glial activation, involving increased expression of TLR2 and CB_2 receptors, and the release of proinflammatory cytokines known to directly damage sensory neurons, resulting in mechanical allodynia. These results are consistent with the findings that TLR pathway activation is a key initiating component of the neuroinflammatory process,[105] and mice with TLR2-deficient microglia have reduced neuroinflammatory responses.[106] Activation of TLRs are also reported to lead to ERK1/2 phosphorylation,[107] and TLR-induced mitogen-activated protein kinases (MAPKs) have been found to be crucial for cytokine production by innate immune cells.[108] Importantly, we have also shown that this process could be prevented by the administration of a CB_2 agonist (MDA7) when given proximal to paclitaxel administration. Moreover, gene expression analyses suggested MDA7 administration was associated with blunted paclitaxel-induced increases in TLR2 and cytokine(s) expression.

The present study focuses on the spinal mechanism underlying paclitaxel-induced mechanical allodynia in the dorsal horn, the primary site for the integration of nociceptive information.[109] There is evidence, however, for the association between paclitaxel-induced allodynia and peripheral sensory neuron mitochondrial dysfunction.[110] Although acetyl L-carnitine, a naturally occurring amino acid derivative, has been shown to ameliorate paclitaxel-induced allodynia and decrease the incidence of swollen and vacuolated mitochondria in C-fibers (but not in A-fibers) in rodents,[111] it did not show superiority to placebo when used for treatment of Human Immunodeficiency Virus-associated sensory neuropathy in randomized controlled clinical trials.[10] Superoxide produced from mitochondrial oxidative phosphorylation is considered the major source of reactive oxygen species in neurons and global inhibition of reactive oxygen species has been shown to ameliorate paclitaxel-induced mechanical allodynia, whereas selective inhibition of superoxide radicals was ineffective.[112]

The present study has several clinical implications. The use of high paclitaxel doses and higher intensity schedules is associated with higher response rates and longer response durations in cancer patients.[113] However, with higher cumulative doses and more intense treatment schedules, debilitating neurotoxicity becomes the dose-limiting toxicity in up to 71% of patients.[3,5] Moreover, the risk of developing neuropathy after treatment with

paclitaxel is larger in patients who have preexisting conditions that may cause neuropathy (e.g., diabetes) or who have been treated previously with other neurotoxic chemotherapeutic drugs such as cisplatin and vincristine.[114] The finding that a CB_2 agonist such as MDA7 can prevent the development of paclitaxel-induced mechanical allodynia is a significant advance for several reasons. First, the use of this CB_2 agonist may allow the use of higher doses of chemotherapy or higher intensity treatment durations when one considers a potential therapeutic window for intervention. Second, understanding the mechanistic basis by which CB_2 agonists up-regulate the negative-feedback loop of the neuroinflammatory process and understanding how MDA7 can prevent chemotherapy-induced mechanical allodynia could provide the foundation for the development of new, targeted neuroprotective strategies in several neurologic disorders associated with an excessive neuroinflammatory process.

Supplementary Material

Refer to Web version on PubMed Central for supplementary material.

Acknowledgments

Nancy E. Buckley, PhD, Biological Sciences Department, California State Polytechnic University, Pomona, CA has kindly provided us with $CB_2^{-/-}$ mice.

Funding: This work was supported by start-up funds for MN and grants from the office of Translational Research from MD Anderson Cancer Center. The Pharmacology and Analytical Facility, the Flow Cytometry and Cellular Imaging Facility, the Cancer Genomics Facility, and the Research Animal Support Facility are partially funded through the ‘Core (CSSG) grant from National Cancer Institute [CA16672]’.

References

1. Rowinsky EK, Donehower RC. Paclitaxel (taxol). N Engl J Med. 1995; 332:1004–14. [PubMed: 7885406]
2. Citron ML, Berry DA, Cirrincione C, Hudis C, Winer EP, Gradishar WJ, Davidson NE, Martino S, Livingston R, Ingle JN, Perez EA, Carpenter J, Hurd D, Holland JF, Smith BL, Sartor CI, Leung EH, Abrams J, Schilsky RL, Muss HB, Norton L. Randomized trial of dose-dense versus conventionally scheduled and sequential versus concurrent combination chemotherapy as postoperative adjuvant treatment of node-positive primary breast cancer: first report of Intergroup Trial C9741/Cancer and Leukemia Group B Trial 9741. J Clin Oncol. 2003; 21:1431–9. [PubMed: 12668651]
3. Sarosy G, Kohn E, Stone DA, Rothenberg M, Jacob J, Adamo DO, Ognibene FP, Cunnion RE, Reed E. Phase I study of taxol and granulocyte colony-stimulating factor in patients with refractory ovarian cancer. J Clin Oncol. 1992; 10:1165–70. [PubMed: 1376773]
4. Scripture CD, Figg WD, Sparreboom A. Peripheral neuropathy induced by paclitaxel: recent insights and future perspectives. Curr neuropharmacol. 2006; 4:165–72. [PubMed: 18615126]
5. Postma TJ, Vermorken JB, Liefting AJ, Pinedo HM, Heimans JJ. Paclitaxel-induced neuropathy. Ann Oncol. 1995; 6:489–94. [PubMed: 7669713]
6. Argyriou AA, Koltzenburg M, Polychronopoulos P, Papapetropoulos S, Kalofonos HP. Peripheral nerve damage associated with administration of taxanes in patients with cancer. Crit Rev Oncol Hematol. 2008; 66:218–28. [PubMed: 18329278]
7. Jensen MP, Chodroff MJ, Dworkin RH. The impact of neuropathic pain on health-related quality of life: Review and implications. Neurology. 2007; 68:1178–82. [PubMed: 17420400]
8. Morello CM, Leckband SG, Stoner CP, Moorhouse DF, Sahagian GA. Randomized double-blind study comparing the efficacy of gabapentin with amitriptyline on diabetic peripheral neuropathy pain. Arch Intern Med. 1999; 159:1931–7. [PubMed: 10493324]
9. Steinman MA, Bero LA, Chren MM, Landefeld CS. Narrative review: the promotion of gabapentin: an analysis of internal industry documents. Ann Intern Med. 2006; 145:284–93. [PubMed: 16908919]

10. Phillips TJ, Cherry CL, Cox S, Marshall SJ, Rice AS. Pharmacological treatment of painful HIV-associated sensory neuropathy: a systematic review and meta-analysis of randomised controlled trials. PLoS One. 2010; 5:e14433. [PubMed: 21203440]
11. Openshaw H, Beamon K, Synold TW, Longmate J, Slatkin NE, Doroshow JH, Forman S, Margolin K, Morgan R, Shibata S, Somlo G. Neurophysiological Study of Peripheral Neuropathy after High-Dose Paclitaxel: Lack of Neuroprotective Effect of Amifostine. Clin Cancer Res. 2004; 10:461–7. [PubMed: 14760066]
12. Jacobson SD, Loprinzi CL, Sloan JA, Wilke JL, Novotny PJ, Okuno SH, Jatoi A, Moynihan TJ. Glutamine does not prevent paclitaxel-associated myalgias and arthralgias. J Support Oncol. 2003; 1:274–8. [PubMed: 15334869]
13. Davis ID, Kiers L, MacGregor L, Quinn M, Arezzo J, Green M, Rosenthal M, Chia M, Michael M, Bartley P, Harrison L, Daly M. A Randomized, Double-Blinded, Placebo-Controlled Phase II Trial of Recombinant Human Leukemia Inhibitory Factor (rhuLIF, Emfilermin, AM424) to Prevent Chemotherapy-Induced Peripheral Neuropathy. Clin Cancer Res. 2005; 11:1890–8. [PubMed: 15756015]
14. Rosenzweig MQ, Bender CM, Lucke JP, Yasko JM, Brufsky AM. The decision to prematurely terminate a trial of R-HuEPO due to thrombotic events. J Pain Symptom Manage. 2004; 27:185–90. [PubMed: 15157043]
15. Henke M, Laszig R, Rübe C, Schäfer U, Haase K-D, Schilcher B, Mose S, Beer KT, Burger U, Dougherty C, Frommhold H. Erythropoietin to treat head and neck cancer patients with anaemia undergoing radiotherapy: randomised, double-blind, placebo-controlled trial. The Lancet. 2003; 362:1255–60.
16. Bohlius J, Schmidlin K, Brillant C, Schwarzer G, Trelle S, Seidenfeld J, Zwahlen M, Clarke MJ, Weingart O, Kluge S, Piper M, Napoli M, Rades D, Steensma D, Djulbegovic B, Fey MF, Ray-Coquard I, Moebus V, Thomas G, Untch M, Schumacher M, Egger M, Engert A. Erythropoietin or Darbepoetin for patients with cancer--meta-analysis based on individual patient data. Cochrane database of systematic reviews. 2009:CD007303.
17. Verstappen CC, Heimans JJ, Hoekman K, Postma TJ. Neurotoxic complications of chemotherapy in patients with cancer: clinical signs and optimal management. Drugs. 2003; 63:1549–63. [PubMed: 12887262]
18. Bettoni I, Comelli F, Rossini C, Granucci F, Giagnoni G, Peri F, Costa B. Glial TLR4 receptor as new target to treat neuropathic pain: efficacy of a new receptor antagonist in a model of peripheral nerve injury in mice. Glia. 2008; 56:1312–9. [PubMed: 18615568]
19. Yoon HJ, Jeon SB, Kim IH, Park EJ. Regulation of TLR2 expression by prostaglandins in brain glia. J Immunol. 2008; 180:8400–9. [PubMed: 18523308]
20. Akira S, Takeda K. Toll-like receptor signalling. Nat Rev Immunol. 2004; 4:499–511. [PubMed: 15229469]
21. Lehnardt S, Massillon L, Follett P, Jensen FE, Ratan R, Rosenberg PA, Volpe JJ, Vartanian T. Activation of innate immunity in the CNS triggers neurodegeneration through a Toll-like receptor 4-dependent pathway. Proc Natl Acad Sci U S A. 2003; 100:8514–9. [PubMed: 12824464]
22. Kawasaki K, Akashi S, Shimazu R, Yoshida T, Miyake K, Nishijima M. Mouse toll-like receptor 4.MD-2 complex mediates lipopolysaccharide-mimetic signal transduction by Taxol. J Biol Chem. 2000; 275:2251–4. [PubMed: 10644670]
23. Byrd-Leifer CA, Block EF, Takeda K, Akira S, Ding A. The role of MyD88 and TLR4 in the LPS-mimetic activity of Taxol. Eur J Immunol. 2001; 31:2448–57. [PubMed: 11500829]
24. Scholz J, Woolf CJ. The neuropathic pain triad: neurons, immune cells and glia. Nat Neurosci. 2007; 10:1361–8. [PubMed: 17965656]
25. Peters CM, Jimenez-Andrade JM, Jonas BM, Sevcik MA, Koewler NJ, Ghilardi JR, Wong GY, Mantyh PW. Intravenous paclitaxel administration in the rat induces a peripheral sensory neuropathy characterized by macrophage infiltration and injury to sensory neurons and their supporting cells. Exp Neurol. 2007; 203:42–54. [PubMed: 17005179]
26. Peters CM, Jimenez-Andrade JM, Kuskowski MA, Ghilardi JR, Mantyh PW. An evolving cellular pathology occurs in dorsal root ganglia, peripheral nerve and spinal cord following intravenous administration of paclitaxel in the rat. Brain Res. 2007; 1168:46–59. [PubMed: 17698044]

27. Block ML, Zecca L, Hong J-S. Microglia-mediated neurotoxicity: uncovering the molecular mechanisms. Nat Rev Neurosci. 2007; 8:57–69. [PubMed: 17180163]
28. Giulian D, Vaca K, Corpuz M. Brain glia release factors with opposing actions upon neuronal survival. J Neurosci. 1993; 13:29–37. [PubMed: 8423475]
29. Guo W, Wang H, Watanabe M, Shimizu K, Zou S, LaGraize SC, Wei F, Dubner R, Ren K. Glial-cytokine-neuronal interactions underlying the mechanisms of persistent pain. J Neurosci. 2007; 27:6006–18. [PubMed: 17537972]
30. Hutchinson MR, Zhang Y, Brown K, Coats BD, Shridhar M, Sholar PW, Patel SJ, Crysdale NY, Harrison JA, Maier SF, Rice KC, Watkins LR. Non-stereoselective reversal of neuropathic pain by naloxone and naltrexone: involvement of toll-like receptor 4 (TLR4). Eur J Neurosci. 2008; 28:20–9. [PubMed: 18662331]
31. Munro S, Thomas KL, Abu-Shaar M. Molecular characterization of a peripheral receptor for cannabinoids. Nature. 1993; 365:61–5. [PubMed: 7689702]
32. Van Sickle MD, Duncan M, Kingsley PJ, Mouihate A, Urbani P, Mackie K, Stella N, Makriyannis A, Piomelli D, Davison JS, Marnett LJ, Di Marzo V, Pittman QJ, Patel KD, Sharkey KA. Identification and Functional Characterization of Brainstem Cannabinoid CB2 Receptors. Science. 2005; 310:329–32. [PubMed: 16224028]
33. McPartland JM. Phylogenomic and chemotaxonomic analysis of the endocannabinoid system. Brain Res Rev. 2004; 45:18–29. [PubMed: 15063097]
34. Ahn K, McKinney MK, Cravatt BF. Enzymatic Pathways That Regulate Endocannabinoid Signaling in the Nervous System. Chem Rev. 2008; 108:1687–707. [PubMed: 18429637]
35. Felder CC, Joyce KE, Briley EM, Mansouri J, Mackie K, Blond O, Lai Y, Ma AL, Mitchell RL. Comparison of the pharmacology and signal transduction of the human cannabinoid CB1 and CB2 receptors. Mol Pharmacol. 1995; 48:443–50. [PubMed: 7565624]
36. Sugiura T, Kodaka T, Nakane S, Miyashita T, Kondo S, Suhara Y, Takayama H, Waku K, Seki C, Baba N, Ishima Y. Evidence that the cannabinoid CB1 receptor is a 2-arachidonoylglycerol receptor. Structure-activity relationship of 2-arachidonoylglycerol, ether-linked analogues, and related compounds. J Biol Chem. 1999; 274:2794–801. [PubMed: 9915812]
37. Sugiura T, Kondo S, Kishimoto S, Miyashita T, Nakane S, Kodaka T, Suhara Y, Takayama H, Waku K. Evidence that 2-arachidonoylglycerol but not N-palmitoylethanolamine or anandamide is the physiological ligand for the cannabinoid CB2 receptor. Comparison of the agonistic activities of various cannabinoid receptor ligands in HL-60 cells. J Biol Chem. 2000; 275:605–12. [PubMed: 10617657]
38. Benito C, Nunez E, Tolon RM, Carrier EJ, Rabano A, Hillard CJ, Romero J. Cannabinoid CB2 receptors and fatty acid amide hydrolase are selectively overexpressed in neuritic plaque-associated glia in Alzheimer's disease brains. J Neurosci. 2003; 23:11136–41. [PubMed: 14657172]
39. Ramirez BG, Blazquez C, Gomez del Pulgar T, Guzman M, de Ceballos ML. Prevention of Alzheimer's disease pathology by cannabinoids: neuroprotection mediated by blockade of microglial activation. J Neurosci. 2005; 25:1904–13. [PubMed: 15728830]
40. Zhang J, Hoffert C, Vu HK, Groblewski T, Ahmad S, O'Donnell D. Induction of CB2 receptor expression in the rat spinal cord of neuropathic but not inflammatory chronic pain models. Eur J Neurosci. 2003; 17:2750–4. [PubMed: 12823482]
41. Romero-Sandoval A, Nutile-McMenemy N, DeLeo JA. Spinal microglial and perivascular cell cannabinoid receptor type 2 activation reduces behavioral hypersensitivity without tolerance after peripheral nerve injury. Anesthesiology. 2008; 108:722–34. [PubMed: 18362605]
42. Beltramo M, Bernardini N, Bertorelli R, Campanella M, Nicolussi E, Fredduzzi S, Reggiani A. CB2 receptor-mediated antihyperalgesia: possible direct involvement of neural mechanisms. Eur J Neurosci. 2006; 23:1530–8. [PubMed: 16553616]
43. Naguib M, Diaz F, Xu J, Astruc-Diaz F, Craig S, Vivas-Mejia P, Brown DL. MDA7: A novel selective agonist for CB2 receptors that prevents allodynia in rat neuropathic pain models. Br J Pharmacol. 2008; 155:1104–16. [PubMed: 18846037]

44. Xu JJ, Diaz P, Astruc-Diaz F, Craig S, Munoz E, Naguib M. Pharmacological characterization of a novel cannabinoid ligand, MDA19, for treatment of neuropathic pain. Anesth Analg. 2010; 111:99–109. [PubMed: 20522703]
45. Racz I, Nadal X, Alferink J, Banos JE, Rehnelt J, Martin M, Pintado B, Gutierrez-Adan A, Sanguino E, Manzanares J, Zimmer A, Maldonado R. Crucial role of CB(2) cannabinoid receptor in the regulation of central immune responses during neuropathic pain. J Neurosci. 2008; 28:12125–35. [PubMed: 19005077]
46. Ehrhart J, Obregon D, Mori T, Hou H, Sun N, Bai Y, Klein T, Fernandez F, Tan J, Shytle RD. Stimulation of cannabinoid receptor 2 (CB2) suppresses microglial activation. J Neuroinflammation. 2005; 2:29. [PubMed: 16343349]
47. Selvarajah D, Gandhi R, Emery CJ, Tesfaye S. Randomized Placebo-Controlled Double-Blind Clinical Trial of Cannabis-Based Medicinal Product (Sativex) in Painful Diabetic Neuropathy. Diabetes Care. 2010; 33:128–30. [PubMed: 19808912]
48. Attal N, Brasseur L, Guirimand D, Clermond-Gnamien S, Atlami S, Bouhassira D. Are oral cannabinoids safe and effective in refractory neuropathic pain? Eur J Pain. 2004; 8:173–7. [PubMed: 14987627]
49. Abrams DI, Jay CA, Shade SB, Vizoso H, Reda H, Press S, Kelly ME, Rowbotham MC, Petersen KL. Cannabis in painful HIV-associated sensory neuropathy: a randomized placebo-controlled trial. Neurology. 2007; 68:515–21. [PubMed: 17296917]
50. Nurmikko TJ, Serpell MG, Hoggart B, Toomey PJ, Morlion BJ, Haines D. Sativex successfully treats neuropathic pain characterised by allodynia: a randomised, double-blind, placebo-controlled clinical trial. Pain. 2007; 133:210–20. [PubMed: 17997224]
51. Ibrahim MM, Rude ML, Stagg NJ, Mata HP, Lai J, Vanderah TW, Porreca F, Buckley NE, Makriyannis A, Malan TP Jr. CB2 cannabinoid receptor mediation of antinociception. Pain. 2006; 122:36–42. [PubMed: 16563625]
52. Cox ML, Haller VL, Welch SP. The antinociceptive effect of [Delta]9-tetrahydrocannabinol in the arthritic rat involves the CB2 cannabinoid receptor. Eur J Pharmacol. 2007; 570:50–6. [PubMed: 17588560]
53. Guindon J, Hohmann AG. Cannabinoid CB2 receptors: a therapeutic target for the treatment of inflammatory and neuropathic pain. Br J Pharmacol. 2008; 153:319–34. [PubMed: 17994113]
54. Diaz P, Xu JJ, Astruc-Diaz F, Pan H-M, Brown DL, Naguib M. Design and synthesis of a novel series of N-alkyl isatin acylhydrazone derivatives that act as selective CB2 agonists for the treatment of neuropathic pain. J Med Chem. 2008; 51:4932–47. [PubMed: 18666769]
55. Diaz P, Phatak SS, Xu J, Astruc-Diaz F, Cavasotto CN, Naguib M. 6-Methoxy-N-alkyl isatin acylhydrazone derivatives as a novel series of potent selective cannabinoid receptor 2 inverse agonists: design, synthesis, and binding mode prediction. J Med Chem. 2009; 52:433–44. [PubMed: 19115816]
56. Diaz P, Phatak SS, Xu J, Fronczek FR, Astruc-Diaz F, Thompson CM, Cavasotto CN, Naguib M. 2,3-Dihydro-1-benzofuran derivatives as a novel series of potent selective cannabinoid receptor 2 agonists: design, synthesis, and binding mode prediction through ligand-steered modeling. ChemMedChem. 2009; 4:1615–29. [PubMed: 19637157]
57. Buckley NE, McCoy KL, Mezey E, Bonner T, Zimmer A, Felder CC, Glass M, Zimmer A. Immunomodulation by cannabinoids is absent in mice deficient for the cannabinoid CB2 receptor. Eur J Pharmacol. 2000; 396:141–9. [PubMed: 10822068]
58. Polomano RC, Mannes AJ, Clark US, Bennett GJ. A painful peripheral neuropathy in the rat produced by the chemotherapeutic drug, paclitaxel. Pain. 2001; 94:293–304. [PubMed: 11731066]
59. Chaplan SR, Bach FW, Pogrel JW, Chung JM, Yaksh TL. Quantitative assessment of tactile allodynia in the rat paw. J Neurosci Methods. 1994; 53:55–63. [PubMed: 7990513]
60. Dixon W. The up-and-down method for small samples. J Am Stat Assoc. 1965; 60:967–78.
61. Brainin-Mattos J, Smith ND, Malkmus S, Rew Y, Goodman M, Taulane J, Yaksh TL. Cancer-related bone pain is attenuated by a systemically available [delta]-opioid receptor agonist. Pain. 2006; 122:174–81. [PubMed: 16545911]

62. Smyth, GK. Limma: linear models for microarray data.. In: Gentleman, R.; Carey, V.; Dudoit, S.; Irizarry, R.; Huber, W., editors. Bioinformatics and Computational Biology Solutions using R and Bioconductor. Springer; New York: 2005. p. 397-420.
63. Benjamini Y, Drai D, Elmer G, Kafkafi N, Golani I. Controlling the false discovery rate in behavior genetics research. Behav Brain Res. 2001; 125:279–84. [PubMed: 11682119]
64. Benjamini Y, Hochberg Y. Controlling the false discovery rate: a practical and powerful approach to multiple testing. J R Stat Soc Ser B. 1995; 57:289–300.
65. Pounds S, Morris SW. Estimating the occurrence of false positives and false negatives in microarray studies by approximating and partitioning the empirical distribution of p-values. Bioinformatics. 2003; 19:1236–42. [PubMed: 12835267]
66. Giulian D, Baker TJ. Characterization of ameboid microglia isolated from developing mammalian brain. J Neurosci. 1986; 6:2163–78. [PubMed: 3018187]
67. Tham CS, Whitaker J, Luo L, Webb M. Inhibition of microglial fatty acid amide hydrolase modulates LPS stimulated release of inflammatory mediators. FEBS Lett. 2007; 581:2899–904. [PubMed: 17543306]
68. Laird NM, Ware JH. Random-effects models for longitudinal data. Biometrics. 1982; 38:963–74. [PubMed: 7168798]
69. Zhuang ZY. Role of the CX3CR1/p38 MAPK pathway in spinal microglia for the development of neuropathic pain following nerve injury-induced cleavage of fractalkine. Brain Behav Immun. 2007; 21:642–51. [PubMed: 17174525]
70. Mor D, Bembrick AL, Austin PJ, Wyllie PM, Creber NJ, Denyer GS, Keay KA. Anatomically specific patterns of glial activation in the periaqueductal gray of the sub-population of rats showing pain and disability following chronic constriction injury of the sciatic nerve. Neuroscience. 2010; 166:1167–84. [PubMed: 20109535]
71. Eng LF. Glial fibrillary acidic protein (GFAP): the major protein of glial intermediate filaments in differentiated astrocytes. J Neuroimmunol. 1985; 8:203–14. [PubMed: 2409105]
72. Garrison CJ, Dougherty PM, Kajander KC, Carlton SM. Staining of glial fibrillary acidic protein (GFAP) in lumbar spinal cord increases following a sciatic nerve constriction injury. Brain Res. 1991; 565:1–7. [PubMed: 1723019]
73. Martinez-Duncker I, Mollicone R, Candelier JJ, Breton C, Oriol R. A new superfamily of protein-O-fucosyltransferases, alpha2-fucosyltransferases, and alpha6-fucosyltransferases: phylogeny and identification of conserved peptide motifs. Glycobiology. 2003; 13:1C–5C. [PubMed: 12634318]
74. Shi S, Stanley P. Protein O-fucosyltransferase 1 is an essential component of Notch signaling pathways. Proc Natl Acad Sci U S A. 2003; 100:5234–9. [PubMed: 12697902]
75. Malatesta P, Hack MA, Hartfuss E, Kettenmann H, Klinkert W, Kirchhoff F, Götz M. Neuronal or Glial Progeny: Regional Differences in Radial Glia Fate. Neuron. 2003; 37:751–64. [PubMed: 12628166]
76. Cao Q, Lu J, Kaur C, Sivakumar V, Li F, Cheah PS, Dheen ST, Ling E-A. Expression of Notch-1 receptor and its ligands Jagged-1 and Delta-1 in amoeboid microglia in postnatal rat brain and murine BV-2 cells. Glia. 2008; 56:1224–37. [PubMed: 18449946]
77. Trofimova-Griffin ME, Juchau MR. Developmental expression of cytochrome CYP26B1 (P450RAI-2) in human cephalic tissues. Brain Res Dev Brain Res. 2002; 136:175–8.
78. Bowman CC, Rasley A, Tranguch SL, Marriott I. Cultured astrocytes express toll-like receptors for bacterial products. Glia. 2003; 43:281–91. [PubMed: 12898707]
79. Lehnardt S, Lachance C, Patrizi S, Lefebvre S, Follett PL, Jensen FE, Rosenberg PA, Volpe JJ, Vartanian T. The toll-like receptor TLR4 is necessary for lipopolysaccharide-induced oligodendrocyte injury in the CNS. J Neurosci. 2002; 22:2478–86. [PubMed: 11923412]
80. Yang RB, Mark MR, Gray A, Huang A, Xie MH, Zhang M, Goddard A, Wood WI, Gurney AL, Godowski PJ. Toll-like receptor-2 mediates lipopolysaccharide-induced cellular signalling. Nature. 1998; 395:284–8. [PubMed: 9751057]
81. Kawasaki K, Akashi S, Shimazu R, Yoshida T, Miyake K, Nishijima M. Involvement of TLR4/MD-2 complex in species-specific lipopolysaccharide-mimetic signal transduction by Taxol. J Endotoxin Res. 2001; 7:232–6. [PubMed: 11581576]

82. Mukhopadhyay S, Das S, Williams EA, Moore D, Jones JD, Zahm DS, Ndengele MM, Lechner AJ, Howlett AC. Lipopolysaccharide and cyclic AMP regulation of CB(2) cannabinoid receptor levels in rat brain and mouse RAW 264.7 macrophages. J Neuroimmunol. 2006; 181:82–92. [PubMed: 17045344]
83. Shoemaker JL, Ruckle MB, Mayeux PR, Prather PL. Agonist-directed trafficking of response by endocannabinoids acting at CB2 receptors. J Pharmacol Exp Ther. 2005; 315:828–38. [PubMed: 16081674]
84. Yang CP, Horwitz SB. Distinct mechanisms of taxol-induced serine phosphorylation of the 66-kDa Shc isoform in A549 and RAW 264.7 cells. Biochim Biophys Acta. 2002; 1590:76–83. [PubMed: 12063170]
85. Bolognini D, Cascio MG, Parolaro D, Pertwee RG. AM630 behaves as a protean ligand at the human cannabinoid CB(2) receptor. Br J Pharmacol. 2011
86. Guzman M. Cannabinoids: potential anticancer agents. Nat Rev Cancer. 2003; 3:745–55. [PubMed: 14570037]
87. Alexander A, Smith PF, Rosengren RJ. Cannabinoids in the treatment of cancer. Cancer Lett. 2009; 285:6–12. [PubMed: 19442435]
88. Svensson M, Eriksson NP, Aldskogius H. Evidence for activation of astrocytes via reactive microglial cells following hypoglossal nerve transection. J Neurosci Res. 1993; 35:373–81. [PubMed: 8360946]
89. Tanga FY, Nutile-McMenemy N, DeLeo JA. The CNS role of Toll-like receptor 4 in innate neuroimmunity and painful neuropathy. Proc Natl Acad Sci U S A. 2005; 102:5856–61. [PubMed: 15809417]
90. Ji RR, Kawasaki Y, Zhuang ZY, Wen YR, Decosterd I. Possible role of spinal astrocytes in maintaining chronic pain sensitization: review of current evidence with focus on bFGF/JNK pathway. Neuron Glia Biol. 2006; 2:259–69. [PubMed: 17710215]
91. Flatters SJ, Bennett GJ. Ethosuximide reverses paclitaxel- and vincristine-induced painful peripheral neuropathy. Pain. 2004; 109:150–61. [PubMed: 15082137]
92. Smith SB, Crager SE, Mogil JS. Paclitaxel-induced neuropathic hypersensitivity in mice: responses in 10 inbred mouse strains. Life Sci. 2004; 74:2593–604. [PubMed: 15041441]
93. Ledeboer A, Jekich BM, Sloane EM, Mahoney JH, Langer SJ, Milligan ED, Martin D, Maier SF, Johnson KW, Leinwand LA, Chavez RA, Watkins LR. Intrathecal interleukin-10 gene therapy attenuates paclitaxel-induced mechanical allodynia and proinflammatory cytokine expression in dorsal root ganglia in rats. Brain Behav Immun. 2007; 21:686–98. [PubMed: 17174526]
94. Zheng FY, Xiao WH, Bennett GJ. The response of spinal microglia to chemotherapy-evoked painful peripheral neuropathies is distinct from that evoked by traumatic nerve injuries. Neuroscience. 2011; 176:447–54. [PubMed: 21195745]
95. Barton GM, Medzhitov R. Toll-like receptor signaling pathways. Science. 2003; 300:1524–5. [PubMed: 12791976]
96. McKimmie CS, Fazakerley JK. In response to pathogens, glial cells dynamically and differentially regulate Toll-like receptor gene expression. J Neuroimmunol. 2005; 169:116–25. [PubMed: 16146656]
97. Kim D, Kim MA, Cho IH, Kim MS, Lee S, Jo EK, Choi SY, Park K, Kim JS, Akira S, Na HS, Oh SB, Lee SJ. A critical role of toll-like receptor 2 in nerve injury-induced spinal cord glial cell activation and pain hypersensitivity. J Biol Chem. 2007; 282:14975–83. [PubMed: 17355971]
98. Xu Q, Garraway SM, Weyerbacher AR, Shin SJ, Inturrisi CE. Activation of the neuronal extracellular signal-regulated kinase 2 in the spinal cord dorsal horn is required for complete Freund's adjuvant-induced pain hypersensitivity. J Neurosci. 2008; 28:14087–96. [PubMed: 19109491]
99. Ji RR, Baba H, Brenner GJ, Woolf CJ. Nociceptive-specific activation of ERK in spinal neurons contributes to pain hypersensitivity. Nat Neurosci. 1999; 2:1114–9. [PubMed: 10570489]
100. Ji RR, Befort K, Brenner GJ, Woolf CJ. ERK MAP kinase activation in superficial spinal cord neurons induces prodynorphin and NK-1 upregulation and contributes to persistent inflammatory pain hypersensitivity. J Neurosci. 2002; 22:478–85. [PubMed: 11784793]

101. Zhuang ZY, Gerner P, Woolf CJ, Ji RR. ERK is sequentially activated in neurons, microglia, and astrocytes by spinal nerve ligation and contributes to mechanical allodynia in this neuropathic pain model. Pain. 2005; 114:149–59. [PubMed: 15733640]
102. Bhat NR, Zhang P, Lee JC, Hogan EL. Extracellular signal-regulated kinase and p38 subgroups of mitogen-activated protein kinases regulate inducible nitric oxide synthase and tumor necrosis factor-alpha gene expression in endotoxin-stimulated primary glial cultures. J Neurosci. 1998; 18:1633–41. [PubMed: 9464988]
103. Sweeney SE, Firestein GS. Mitogen activated protein kinase inhibitors: where are we now and where are we going? Ann Rheum Dis. 2006; 65(Suppl 3):iii83–8. [PubMed: 17038480]
104. Eljaschewitsch E, Witting A, Mawrin C, Lee T, Schmidt PM, Wolf S, Hoertnagl H, Raine CS, Schneider-Stock R, Nitsch R, Ullrich O. The endocannabinoid anandamide protects neurons during CNS inflammation by induction of MKP-1 in microglial cells. Neuron. 2006; 49:67–79. [PubMed: 16387640]
105. Sun H, Gong S, Carmody RJ, Hilliard A, Li L, Sun J, Kong L, Xu L, Hilliard B, Hu S, Shen H, Yang X, Chen YH. TIPE2, a negative regulator of innate and adaptive immunity that maintains immune homeostasis. Cell. 2008; 133:415–26. [PubMed: 18455983]
106. Hoffmann O, Braun JS, Becker D, Halle A, Freyer D, Dagand E, Lehnardt S, Weber JR. TLR2 Mediates Neuroinflammation and Neuronal Damage. J Immunol. 2007; 178:6476–81. [PubMed: 17475877]
107. Martin M, Michalek SM, Katz J. Role of innate immune factors in the adjuvant activity of monophosphoryl lipid A. Infect Immun. 2003; 71:2498–507. [PubMed: 12704121]
108. Wang X, Meng X, Kuhlman JR, Nelin LD, Nicol KK, English BK, Liu Y. Knockout of Mkp-1 enhances the host inflammatory responses to gram-positive bacteria. J Immunol. 2007; 178:5312–20. [PubMed: 17404316]
109. Millan MJ. The induction of pain: an integrative review. Prog Neurobiol. 1999; 57:1–164. [PubMed: 9987804]
110. Flatters SJ, Bennett GJ. Studies of peripheral sensory nerves in paclitaxel-induced painful peripheral neuropathy: evidence for mitochondrial dysfunction. Pain. 2006; 122:245–57. [PubMed: 16530964]
111. Jin HW, Flatters SJ, Xiao WH, Mulhern HL, Bennett GJ. Prevention of paclitaxel-evoked painful peripheral neuropathy by acetyl-L-carnitine: effects on axonal mitochondria, sensory nerve fiber terminal arbors, and cutaneous Langerhans cells. Exp Neurol. 2008; 210:229–37. [PubMed: 18078936]
112. Fidanboylu M, Griffiths LA, Flatters SJ. Global Inhibition of Reactive Oxygen Species (ROS) Inhibits Paclitaxel-Induced Painful Peripheral Neuropathy. PLoS One. 2011; 6:e25212. [PubMed: 21966458]
113. Kohn EC, Sarosy G, Bicher A, Link C, Christian M, Steinberg SM, Rothenberg M, Adamo DO, Davis P, Ognibene FP, Cunnion RE, Reed E. Dose-intense taxol: high response rate in patients with platinum-resistant recurrent ovarian cancer. J Natl Cancer Inst. 1994; 86:18–24. [PubMed: 7505830]
114. Pace A, Bove L, Aloe A, Nardi M, Pietrangeli A, Calabresi F, Innocenti P, Jandolo B. Paclitaxel neurotoxicity: clinical and neurophysiological study of 23 patients. Ital J Neurol Sci. 1997; 18:73–9. [PubMed: 9239526]

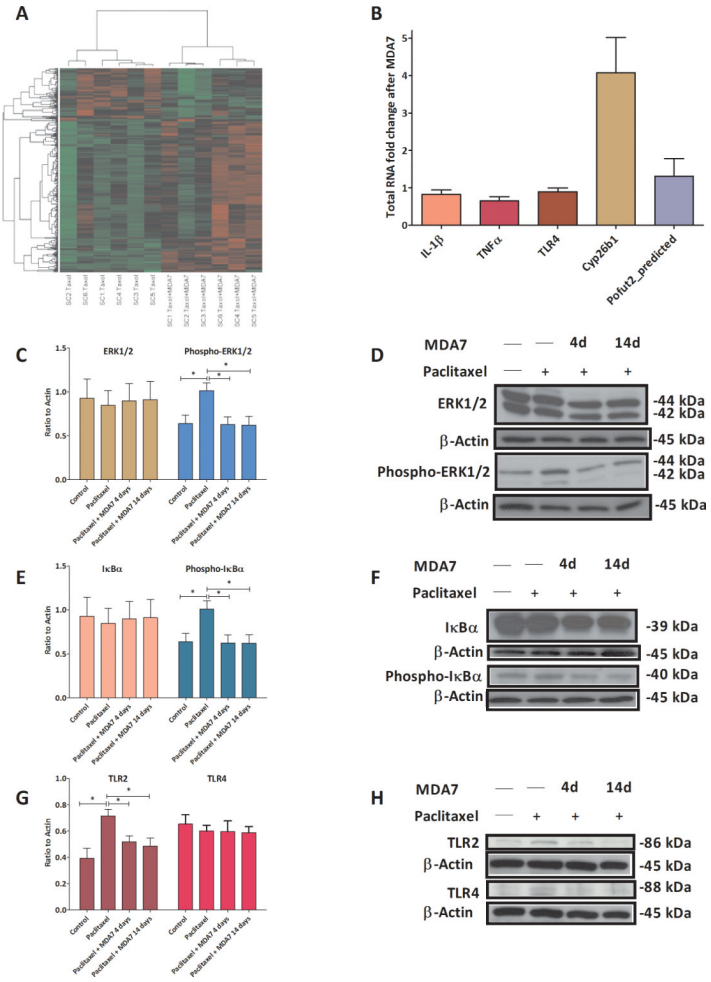

Fig. 1.

(A) Prevention of paclitaxel-induced mechanical allodynia in rats ($n = 6$ in all groups except vehicle control, $n = 4$). Treatment with paclitaxel + MDA7 for 14 days resulted in significant differences ($P < 0.001$) from paclitaxel alone on days 5-28, whereas treatment with paclitaxel + MDA7 for only 4 days resulted in significant differences ($P < 0.01$) on days 5-12 only. **(B)** Confocal images of CD11b immunoreactivity in various groups of rats. *Top*, immunofluorescence staining intensity patterns of each section. **(C)** Analysis of CD11b immunofluorescence intensity by Metamorph (5-6 sections) showed that the paclitaxel + MDA7 14 days group had significantly less immunofluorescence integrated intensity than did the paclitaxel only and paclitaxel + MDA7 4 days groups **(D).** Confocal images of glial fibrillary acidic protein (GFAP) immunoreactivity in various groups of rats. *Top*, immunofluorescence staining intensity patterns of each section. **(E)** Analysis of GFAP immunofluorescence integrated intensity by Metamorph (2-3 sections) showed that the paclitaxel + MDA7 14 days group had significantly less immunofluorescence intensity than the paclitaxel only and paclitaxel + MDA7 4 days groups had. Scale bar = 50μm.

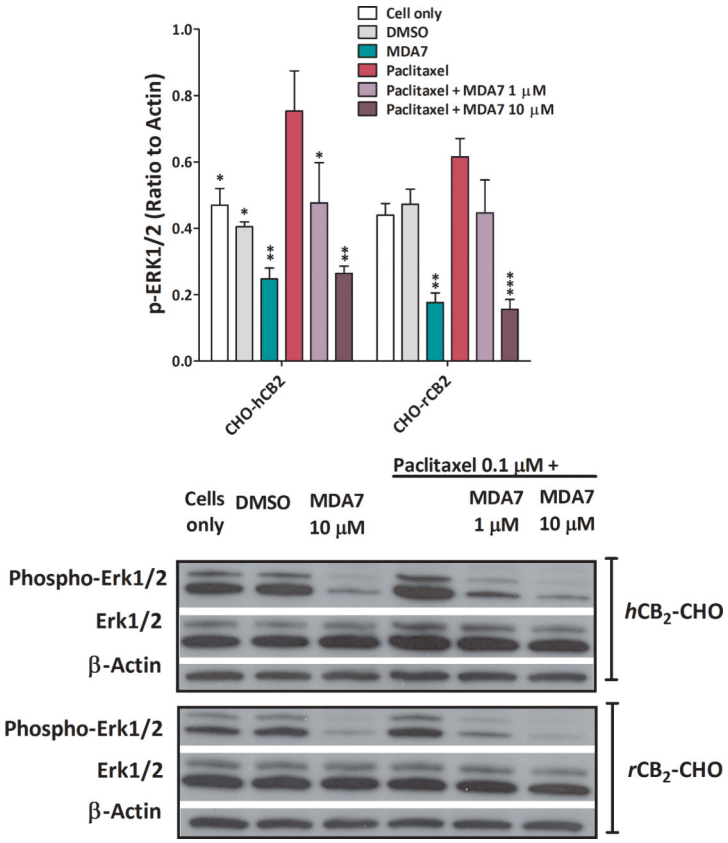

Fig. 2.

The effect of MDA7 is mediated through the Cannabinoid type 2 (CB_2) receptor. MDA7 prevented paclitaxel-induced mechanical allodynia in $CB_2^{+/+}$ **(A)** but not in $CB_2^{-/-}$ mice **(B)**. $^{*}P \leq 0.01$ compared with other groups ($n = 5$ in all groups). $^{+}P \leq 0.05$ compared with paclitaxel 4 days group.

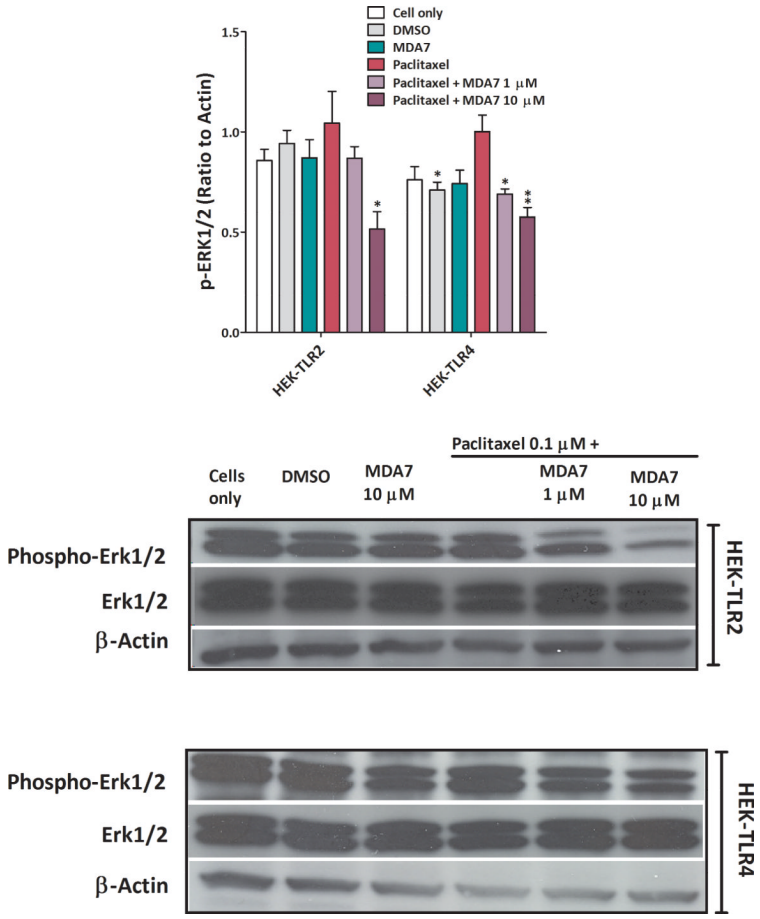

Fig. 3.

(A) Cannabinoid type 2 (CB_2) staining and localization in the lumbar spinal cord dorsal horn laminae I and II. Representative confocal images of CB_2 (*green*) and glial fibrillary acidic protein (GFAP) (*red*). The coregionalization of CB_2 and GFAP in astrocytes is shown in *yellow*. No significant CB_2 expression was observed in the control group, but marked CB_2 expression was observed in the paclitaxel group. CB_2 expression was markedly decreased with MDA7 treatment for 14 days. Scale bar = 50μm. **(B and C)** Paclitaxel treatment significantly increased the CB_2 expression in the lumbar spinal cord, and treatment with MDA7 for 14 days significantly attenuated this upregulated CB_2 expression in the rats treated with paclitaxel.

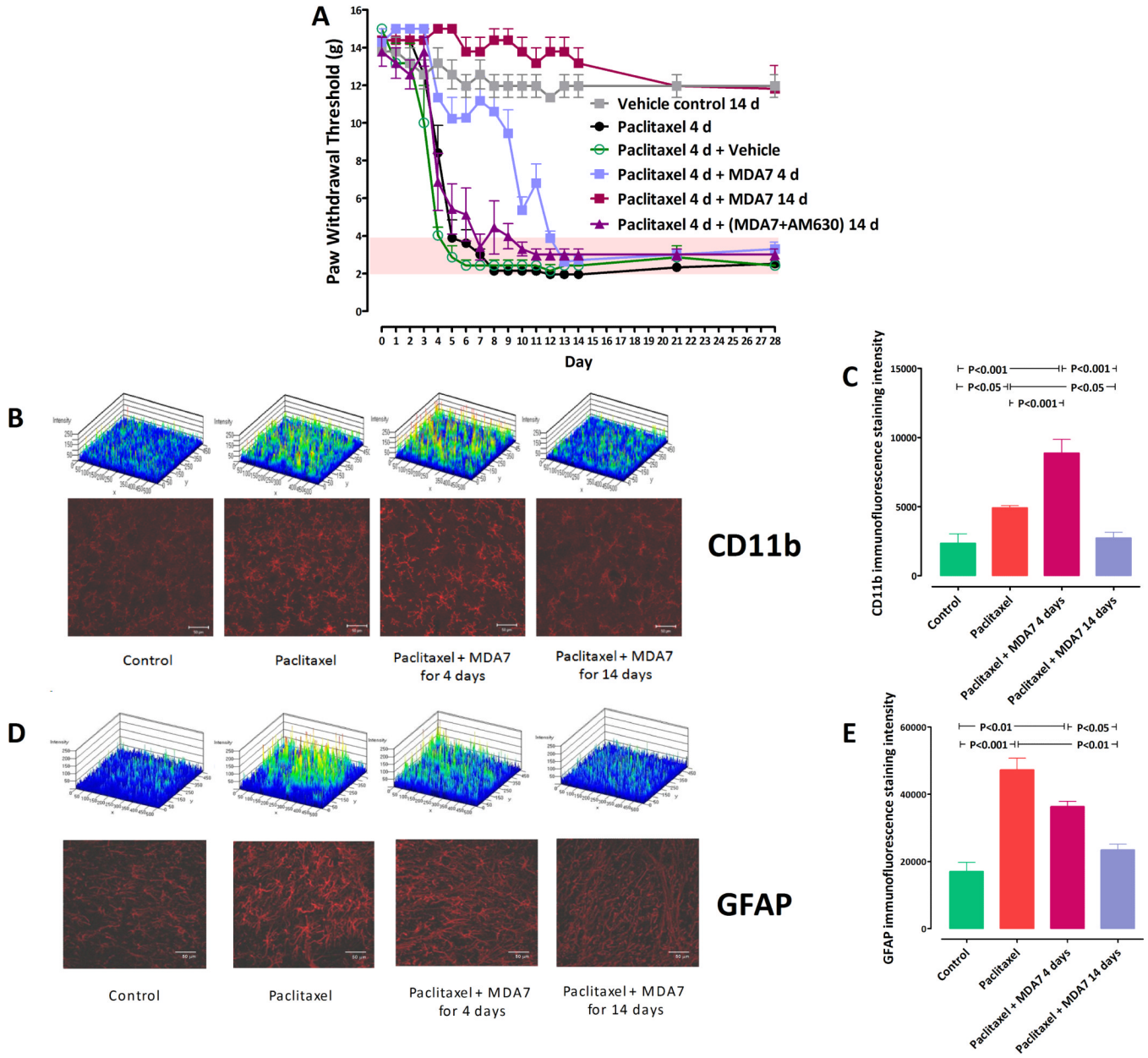

Fig. 4.

(A) Heatmap of the expression intensities in the individual samples of the most significant 384 genes detected on the basis of the threshold of false discovery rate cutoff of 0.005. Hierarchical clustering based on Pearson's correlation coefficient was conducted among the 384 genes. SC = spinal cord. Taxol = paclitaxel. **(B)** Quantitative real-time reverse transcriptase-polymerase chain reaction (qRT–PCR) analysis of total RNA performed in triplicates isolated from all 12 spinal cord samples used in a microarray study (6 from paclitaxel-treated rats and 6 from paclitaxel + MDA7 14 d–treated rats). Data were normalized relative to *Gapdh* and expressed as fold change relative to paclitaxel treatment without MDA7. The RNA fold change matches the trend seen in microarray data. Further, Western blotting analysis revealed that MDA7 treatment for 14 days significantly attenuated the upsurge of phosphorylation of extracellular signal regulated kinase (ERK)1/2 (**C, D**) and IκBα (**E, F**), and down-regulated Toll-like receptors 2 (TLR2) expression (**G,H**) but did not

affect TLR4 (**G, H**) expression in the spinal cord of the rats with paclitaxel treatment. * = $P<0.05$.

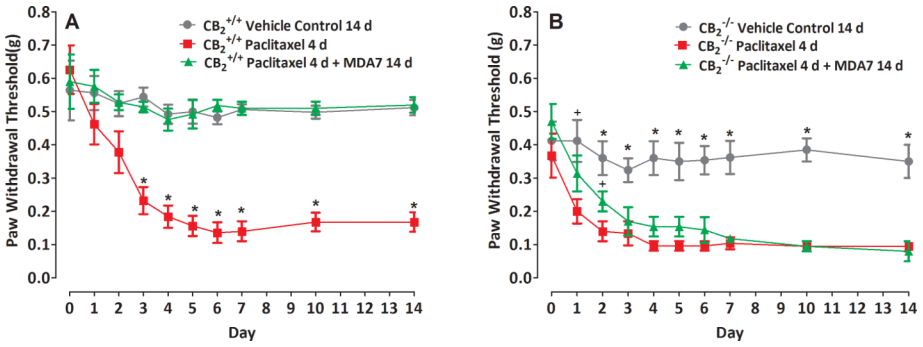

Fig. 5.

MDA7 inhibited lipopolysaccharide (LPS, a Toll-like receptors 4 [TLR4] ligand)- and zymosan (a TLR2 ligand)-induced increases in interleukin (IL)-1β and tumor necrosis factor (TNF)-α secretion. Primary cultured astroglial cells were treated with 5 μM dimethylsulfoxide (DMSO) (solvent), 1.0 μg/ml lipopolysaccharide (LPS), and 100 μg/ml zymosan with or without 10 μM MDA7. Pretreatment with MDA7 significantly inhibited LPS-induced increases in IL-1β (A) and TNF-α secretion (B). Similarly, it also suppressed zymosan-induced increases in IL-1β (A) and TNF-α secretion (B). Arrows indicate that the corresponding TNF-α secretion was below detection level. **(C)** MDA7 attenuated the paclitaxel-induced increase in TLR2 mRNA level in cultured primary astroglial cells. There was no change in TLR4 mRNA level among groups.

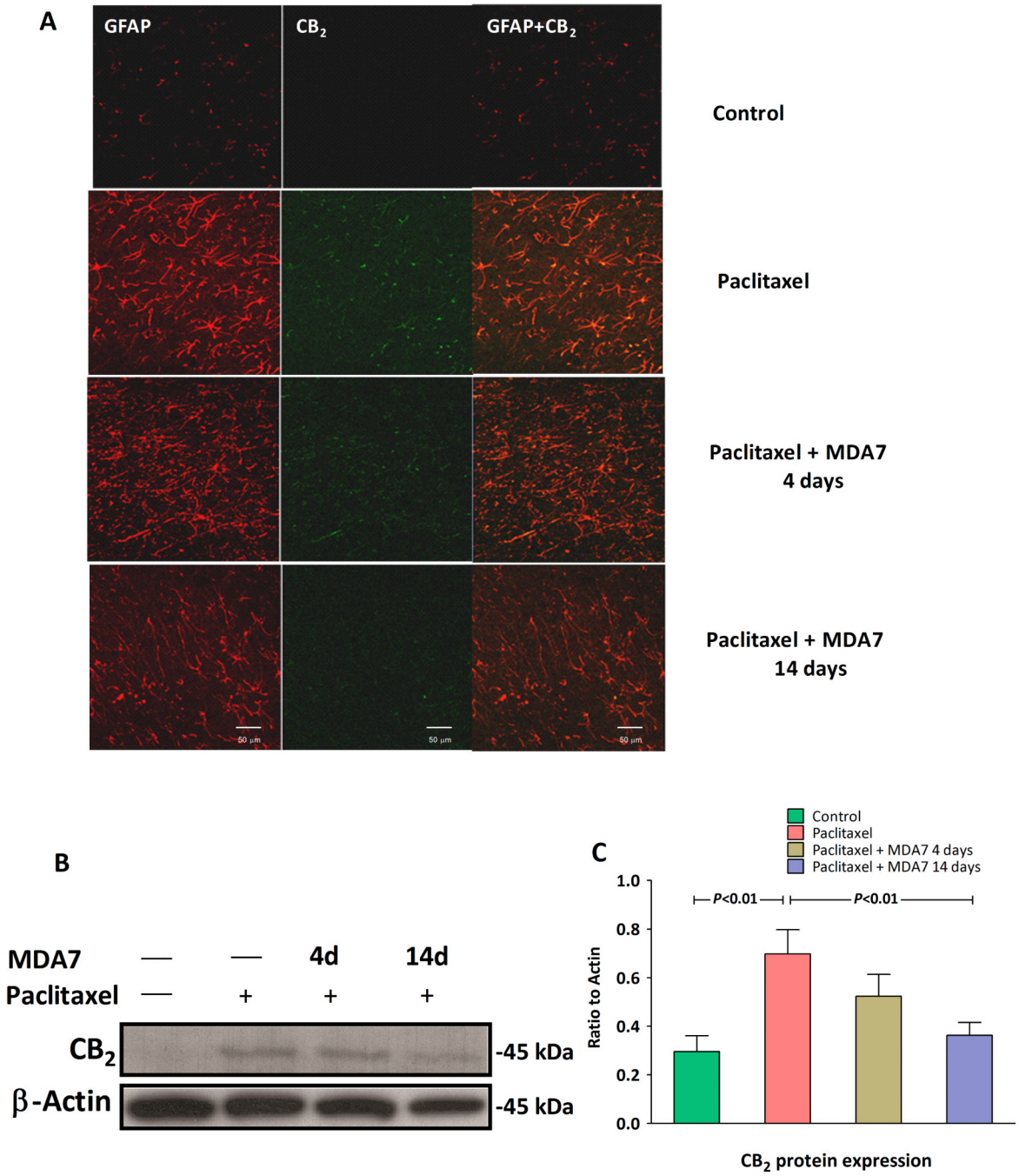

Fig. 6.

MDA7 decreased paclitaxel-induced phosphorylation of extracellular signal regulated kinase (ERK)1/2 in human Cannabinoid type 2 (CB_2) (*h*CB_2) or rat CB_2 (*r*CB_2) receptor-transfected Chinese hamster ovary (CHO) cells. Cells were treated with dimethylsulfoxide (DMSO) (vehicle) and 0.1 μM paclitaxel (15 min) with or without 1 and 10 μM MDA7 (1 h before paclitaxel). Antibodies to ERK1/2 and phosphorylated-ERK1/2 (1:1500, Cell Signaling) were used. *Top*, grouped results to show the suppressive effect of MDA7 on the paclitaxel-induced phosphorylation of ERK1/2 in human CB_2 (*h*CB_2) or rat CB_2 (*r*CB_2) receptor-transfected CHO cells. **P* < 0.05, ***P* < 0.01, ****P* < 0.001 *versus* paclitaxel.

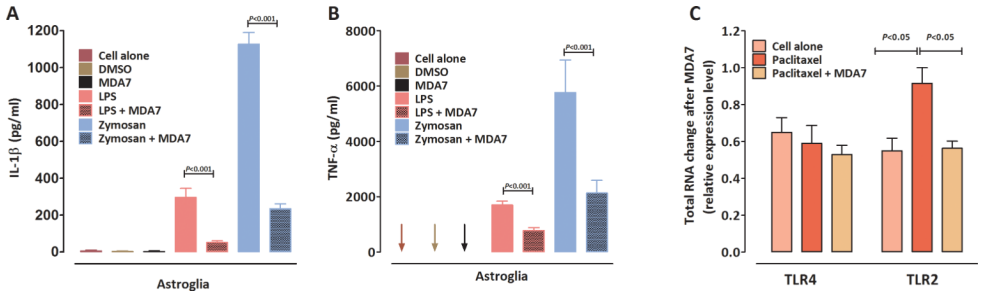

Fig. 7.

MDA7 decreased paclitaxel-induced phosphorylation of extracellular signal regulated kinase (ERK)1/2 in Toll-like receptors (TLR)2- or TLR4-transfected Human Embryonic Kidney (HEK)-293 cells. Cells were treated with dimethylsulfoxide (DMSO) (vehicle) and 0.1 μM paclitaxel (15 min) with or without 1 and 10 μM MDA7 (1 h before paclitaxel). *Top*, grouped results to show the suppressive effect of MDA7 on the paclitaxel-induced phosphorylation of ERK1/2 in TLR2- or TLR4-transfected HEK-293 cells. $*P < 0.05$, $**P < 0.01$ *versus* paclitaxel.

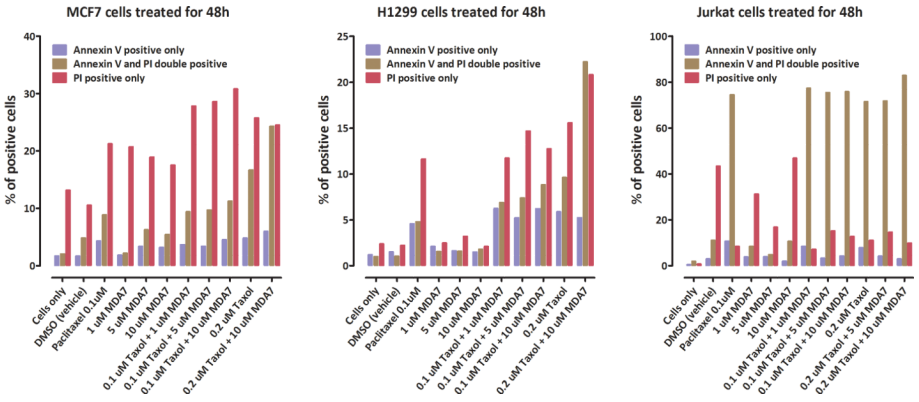

Fig. 8.

Effects of MDA7 on paclitaxel-induced cytotoxicity. MCF7, H1299, and Jurkat cell cultures were treated with MDA7 alone (1, 5, or 10 μM), paclitaxel alone (0.1 or 0.2 μM) or their combination for 48h and then assayed for the degree of cytotoxicity using measures of apoptosis (Annexin V staining) and necrosis (propidium iodide uptake).